

**THE FEASIBILITY OF DEVELOPING AN EMBOSSED
FIBERGLASS FILTER MEDIA PACK FOR AIR
FILTRATION DEVICES**

GOH JENN HSEN

**FACULTY OF ENGINEERING
UNIVERSITY OF MALAYA
KUALA LUMPUR**

2019

**THE FEASIBILITY OF DEVELOPING AN
EMBOSSSED FIBERGLASS FILTER MEDIA PACK FOR
AIR FILTRATION DEVICES**

GOH JENN HSEN

**RESEARCH PROJECT SUBMITTED IN PARTIAL
FULFILMENT OF THE REQUIREMENTS FOR THE
DEGREE OF MASTER IN MECHANICAL
ENGINEERING**

**FACULTY OF ENGINEERING
UNIVERSITY OF MALAYA
KUALA LUMPUR**

2019

UNIVERSITY OF MALAYA
ORIGINAL LITERARY WORK DECLARATION

Name of Candidate : Goh Jenn Hsen
Matric No : KQK170031
Name of Degree : Master in Mechanical Engineering
Title of Research Project : The Feasibility of Developing An Embossed Fiberglass
Filter Media Pack For Air Filtration Devices
Field of Study : Air filtration

I do solemnly and sincerely declare that:

- (1) I am the sole author/writer of this Work;
- (2) This Work is original;
- (3) Any use of any work in which copyright exists was done by way of fair dealing and for permitted purposes and any excerpt or extract from, or reference to or reproduction of any copyright work has been disclosed expressly and sufficiently and the title of the Work and its authorship have been acknowledged in this Work;
- (4) I do not have any actual knowledge nor do I ought reasonably to know that the making of this work constitutes an infringement of any copyright work;
- (5) I hereby assign all and every rights in the copyright to this Work to the University of Malaya ("UM"), who henceforth shall be owner of the copyright in this Work and that any reproduction or use in any form or by any means whatsoever is prohibited without the written consent of UM having been first had and obtained;
- (6) I am fully aware that if in the course of making this Work I have infringed any copyright whether intentionally or otherwise, I may be subject to legal action or any other action as may be determined by UM.

Candidate's Signature

Date: 29/01/2020

Subscribed and solemnly declared before,

Witness's Signature

Date:

Name :

Designation :

THE FEASIBILITY OF DEVELOPING AN EMBOSSED FIBERGLASS FILTER MEDIA PACK FOR AIR FILTRATION DEVICES

ABSTRACT

As industrial technology continues to improve at an ever-increasing rate, this advancement comes at the expense of our environment, and more namely to the air quality. Consequently, the field of air filtration has garnered increasing attention and the demand for better air filtration devices has increased accordingly as well. An air filtration device is able to remove pollutants from an air stream. At the time of writing, the most commonly used air filtration medium is Fiberglass. Air filters with fiberglass medium has been commercially available since the 1990s and thus much development has been made to improve its performance. It is already known that pleating a Fiberglass media to form a media pack is able to decrease the air flow resistance of an air filter and increase the dust holding capacity of the air filter. To further improve on this, it was proposed to develop a filter media pack with an emboss design. This work aims to study the feasibility of developing such an air filter. With the aid of Computation Fluid Dynamic (CFD) simulations, the performance of a media pack with emboss design is predicted and found to have lower resistance to air flow and higher dust holding capacity as compared to an equivalent specification air filter. In addition, it was found that for a fiberglass media with 0.5mm thickness and 250 Pa air flow resistance at 0.53 cm/s air velocity, the optimum media pack dimensions are 120 mm Pleat Depth with Pleat Density of 6 Pleats Per Inch. Furthermore, cost analysis was performed to evaluate the Return of Investment of producing an air filter with embossed media pack. It was found that there is potential for high Return of Investment and thus it is feasible to develop an air filter with embossed fiberglass media pack.

THE FEASIBILITY OF DEVELOPING AN EMBOSSED FIBERGLASS FILTER MEDIA PACK FOR AIR FILTRATION DEVICES

ABSTRAK

Dengan kemajuan teknologi perindustrian, keadaan persekitaran kita makin diabaikan, dan terutama lagi kualiti udara. Akibatnya, bidang penapisan udara makin penting dan keperluan untuk peranti penapisan udara yang lebih baik makin meningkat sewajarnya. Peranti penapisan udara mampu menapis kotoran daripada aliran udara. Kini, medium penapisan udara yang paling biasa digunakan ialah gentian kaca. Penapis udara dengan medium gentian kaca telah tersedia secara komersial sejak tahun 1990-an dan oleh itu banyak penyelidikan telah dijalankan untuk meningkatkan prestasinya. Adalah diketahui bahawa media gentian kaca boleh dilipatkan untuk membentuk pek media bagi mengurangkan ketahanan aliran udara penapis udara dan meningkatkan kapasiti penahan debu penapis udara. Untuk mempertingkatkan lagi ini, adalah dicadangkan untuk menyelidik pek media penapis dengan reka bentuk timbul. Kerja ini bertujuan untuk mengkaji kefaedah untuk membuat penapis udara sedemikian. Dengan bantuan simulasi Fluida Dynamik (CFD), prestasi pek media dengan reka bentuk timbul diramalkan mempunyai daya tahan yang lebih rendah terhadap aliran udara dan kapasiti pegangan debu yang lebih tinggi berbanding penapis udara spesifikasi setara. Di samping itu, didapati bahawa untuk media gentian kaca dengan ketebalan 0.5mm dan rintangan aliran udara 250 Pa pada kelajuan udara 0.53 cm / s, dimensi pek media optimum ialah 120 mm tinggi dan 6 kali lipat dalam seinchi. Selain itu, analisis kos dilakukan untuk menilai Pulangan Pelaburan untuk menghasilkan penapis udara dengan pek media timbul. Telah didapati berpotensi untuk Pulangan Pelaburan yang tinggi dan oleh itu, adalah berfaedah untuk menghasilkan penapis udara dengan pek media gentian kaca yang timbul.

ACKNOWLEDGEMENTS

I would like to express my sincere thanks to my project supervisor, Professor Yau Yat Huang, for his support throughout the course of this study. Besides, I would also like to thank my family and friends for their encouragement and moral support throughout my studies.

University of Malaya

TABLE OF CONTENTS

Abstract	iii
Abstrak	iv
Acknowledgements	1
Table of Contents	2
List of Figures	5
List of Tables.....	7
CHAPTER 1: INTRODUCTION.....	8
1.1 Background.....	8
1.2 Problem Statements	9
1.3 Research Questions.....	9
1.4 Aim and Objectives	10
1.5 Scope and Limitations	10
1.6 Outlines of the Thesis	10
CHAPTER 2: LITERATURE REVIEW.....	12
2.1 Introduction.....	12
2.2 Air Filter Performances	12
2.2.1 Pressure Drop	12
2.2.2 Filtration Efficiency	13
2.2.3 Dust Holding Capacity	14
2.3 Classifications of Filters	16
2.4 Common Air Filtration Methods	17
2.4.1 Barrier Filtration.....	17
2.4.2 Inertial Separation	19

2.4.3	Chemical Adsorption.....	20
2.4.4	Catalysts	21
2.5	CFD Modelling Techniques	22
2.6	Chapter Conclusions.....	24
 CHAPTER 3: RESEARCH METHODOLOGY		25
3.1	Introduction.....	25
3.2	Project Flow.....	25
3.3	Project Timeline.....	26
3.4	CFD Configurations	27
3.4.1	CFD Models	28
3.4.2	Computational Meshes	29
3.5	Chapter Conclusions.....	31
 CHAPTER 4: 2-D CFD SIMULATIONS.....		32
4.1	Introduction.....	32
4.2	Model Validations	32
4.3	Parametric Studies	33
4.3.1	Variation in the Height of the Filter Media.....	33
4.3.2	Variation in the Angle of the Filter Media	35
4.3.3	Variation in the Pleat Density of the Filter Media Pack.....	38
4.3.4	Variation in the Pleat Depth of the Filter Media Pack	41
4.4	Chapter Conclusions.....	44
 CHAPTER 5: 3-D CFD SIMULATIONS.....		45
5.1	Introduction.....	45
5.2	3-D Pleated Filter Media Models	45

5.3	Computational Results for 3-D Simulations.....	48
5.3.1	Ideal Media Pack Model.....	48
5.3.2	Pleated Filter Media Model with Hot-Melt Layers	49
5.3.3	Pleated Filter Media Pack Model with Emboss Design	50
5.4	Discussions on the Filtration Performance of the Various Designs	51
5.5	Chapter Conclusions.....	53
 CHAPTER 6: COST ANALYSIS.....		54
6.1	Introduction.....	54
6.2	Manufacturing Cost	54
6.2.1	Materials Cost.....	54
6.2.2	Manufacturing Process	57
6.3	Improvement of Specifications.....	58
6.4	Return of Investment (ROI).....	60
6.5	Chapter Conclusions.....	61
 CHAPTER 7: CONCLUSIONS AND FUTURE WORK		62
7.1	Conclusions	62
7.2	Recommendations for Future Work	63
	References	64

LIST OF FIGURES

Figure 2.1: Contaminant's particle movements (GmbH, n.d.).....	14
Figure 2.2: The dust holding capacity of a PTFE fibre membrane module at different times of a year (Xu et al., 2018).....	15
Figure 2.3: Schematic diagram of surface filtration (Gopani, n.d.).....	18
Figure 2.4: Depth filtration (Gopani, n.d.).....	18
Figure 2.5: Schematic diagram of inertial separation (Domnița, Bacoțiu, Hoțupan, Popovici, & Kapalo, 2014).....	20
Figure 2.6: chemical adsorber.....	21
Figure 2.7: Ozone catalyst filter.....	21
Figure 3.1: Research flow chart of project.....	26
Figure 3.2: 2-D computational grids with (a) straight media pack, (b) angled media pack, and (c) multiple pleats.....	29
Figure 3.3: 3-D computational grids for pleated filter media model (a) without emboss, (b) with emboss, and (c) with hot melt adhesive layers.....	30
Figure 4.1: (a) Pressure drop and (b) velocity vector of the air flow across a straight filter media sheet.....	32
Figure 4.2: Pressure drop across straight filter media packs with height of (a) 70 mm, (b) 80 mm, (c) 94 mm, (d) 114 mm, and (e) 146 mm.	34
Figure 4.3: Graph of pressure drop predictions against heights of filter media packs....	35
Figure 4.4: Pressure drop across filter media packs with installation angle of (a) 5.5°, (b) 7°, (c) 8.5°, (d) 10°, and (e) 11.5°.	36
Figure 4.5: Velocity vectors of the air flow across filter media pack with installation angle of (a) 5.5°, (b) 7°, (c) 8.5°, (d) 10°, and (e) 11.5°.	37
Figure 4.6: Graph of pressure drop predictions against installation angles of filter media packs.....	38
Figure 4.7: Pressure drop across filter media packs with pleat density of (a) 3, (b) 4, (c) 5, (d) 6, (e) 7, (f) 8, (g) 9, (h) 10, and (i) 11 pleats/inch.	39

Figure 4.8: Velocity vectors of the air flow across filter media pack with pleat density of (a) 3, (b) 4, (c) 5, (d) 6, (e) 7, (f) 8, (g) 9, (h) 10, and (i) 11 pleats/inch.	40
Figure 4.9: Graph of pressure drop predictions against pleat density of filter media packs.	41
Figure 4.10: Pressure drop across filter media packs with pleat depth of (a) 12 mm, (b) 25 mm, (c) 35 mm, (d) 50 mm, (e) 70 mm, (f) 95 mm, (g) 120 mm, (h) 135 mm, and (i) 150 mm.	42
Figure 4.11: Velocity vectors of the air flow across filter media pack with pleat depth of (a) 12 mm, (b) 25 mm, (c) 35 mm, (d) 50 mm, (e) 70 mm, (f) 95 mm, (g) 120 mm, (h) 135 mm, and (i) 150 mm.	43
Figure 4.12: Graph of pressure drop predictions against pleat depth of filter media packs.	44
Figure 5.1: 3-D pleated filter media models (a) of an ideal media pack, (b) a media pack with hot-melt adhesive layer, and (c) with emboss design.	46
Figure 5.2: The 3-D model of the media pack with 2 layers of hotmelt adhesive.	47
Figure 5.3: The 3-D model of the media pack with emboss design.	48
Figure 5.4: (a) Pressure drop and (b) velocity profile predictions across simple pleated filter media model.	49
Figure 5.5: (a) Pressure drop and (b) velocity profile predictions across pleated filter media model with hot-melt layers.	50
Figure 5.6: (a) Pressure drop and (b) velocity profile predictions across pleated filter media model with emboss design.	51
Figure 6.1: Computer Aided Design (CAD) Models of the Media Pack with Hotmelt Layers and Media Pack with Emboss Design.	55
Figure 6.2: Comparison of the Manufacturing Processes to produce an air filter with media pack with hotmelt and media pack with emboss design.	57

LIST OF TABLES

Table 2.1: Filter classifications (Purchas & Sutherland, 2002).	16
Table 3.1: Project schedule.	27
Table 3.2: Details of the computational grids for both 2-D and 3-D simulation studies.	31
Table 5.1: Filter media pack resistance to air flow comparison against the Ideal Media Pack.....	52
Table 6.1: Summary of the Materials Required to Manufacture Air Filters with the Media Pack with Hotmelt Layers and Media Pack with Emboss Design.....	56
Table 6.2: Comparison of the Air Filter with Media Pack with Emboss Design versus Media Pack with Hotmelt Layers.....	60

University of Malaysia

CHAPTER 1: INTRODUCTION

1.1 Background

Air filtration is a vastly expanding field with an increasing importance for both industrial and home use. This has led to a demand to produce better air filtration media to improve the performance of air filters. The main parameters of a filter media are its resistance to the air flow, its ability to capture dust and its dust holding capacity. The correlation between these three parameters are convoluted and a designer would usually have to prioritize either 1 parameter in the expense of the other two parameters. In addition, the cost of the material also plays an important role in selecting the right filter media. Set against this background, Fiberglass is the most commonly used filter media as it is the most cost-effective method to provide an optimum of the three aforementioned parameters. To manufacture a Fiberglass media to capture the finess of dust particle, the fibres has to be fine and closely packed. Then, to reduce the resistance to the air flow, the Fiberglass media are pleated to form a media pack. And lastly, to increase its dust holding capacity, the surface area of the media is required to be maximized. The last-mentioned point is the main focus of this research project. Much research and development has been carried out to explore the optimum specifications of a Fiberglass media pack, and from this know-how, the optimum depth of the pack and pleat density for a given Fiberglass media finess has been determined. The depth of the pack and pleat density directly affects the resistance to air flow of the media pack, while the finess of the Fiberglass directly affects the ability to capture fine dust particles. However, the dust holding capacity, which is directly affected by the total media surface area, is fixed based on the dimensions of the media pack. Hence, to further improve the performance of the filter media, a method to increase the surface area of the filter media without changing the dimensions of the media pack was developed. This can be achieved by embossing the filter media.

1.2 Problem Statements

The existing method to produce air filters with embossed Fiberglass filter media is to specially design a Fiberglass medium that could be embossed. This is done by the Fiberglass medium's manufacturer whereby modifications are made at the manufacturing stage of the Fiberglass media. Thus, air filter manufacturers are required to acquire the Fiberglass media that are readily embossed directly from the Fiberglass manufacturers. This is often too costly and offsets the potential advantages of manufacturing air filters with embossed Fiberglass filter media. Hence, a method to produce embossed Fiberglass media packs from existing Fiberglass media is needed. However, before air manufacturers proceed to develop methods to emboss the Fiberglass filter media, the potential Return of Investment (ROI) of such development must first be evaluated. Consequently, evaluating the amount of improvement in performance of an air filter with an embossed media pack is essential in determining the ROI of developing an emboss media pack. Therefore, there is a necessity to investigate the performances of currently available air filters and the potential improvement of an air filter with embossed Fiberglass media.

1.3 Research Questions

Based on the problem statements depicted in Section 1.2, the following research questions for this project are raised:

- (i) What are the effects of changing the media pack configurations on air filtration performance?
- (ii) Which media pack dimensions provide an optimum air filtration performance?
- (iii) Is developing an embossed media pack filter feasible for commercial purposes?

1.4 Aim and Objectives

This study aims to address problems pertaining to the media pack design of the commercial air filter. The main objectives of this work are to:

- (i) investigate the effects of variation in media pack configurations on the predictions of air flow pressure drop;
- (ii) determine the media pack dimensions for optimum air filtration performance and
- (iii) investigate the feasibility of the developing an embossed media pack filter for commercial purposes.

1.5 Scope and Limitations

The present work focuses on the CFD simulation studies of the air filtration performances under a wide range of filter media pack configurations. The experimental data are obtained from the manufacturer of the filter media pack. Therefore, the research work conducted in this project is restricted by the filter model supplies available in the company.

1.6 Outlines of the Thesis

Chapter 1 outlines the background of this research work as well as defines the objectives and scopes of the study. Following that, a detailed literature review is performed on the various CFD techniques to evaluate the air filter performances and they are reported in Chapter 2. In Chapter 3, the research methodology and project timeline are discussed. Next, the 2-D simulation results of the model validations and parametric studies with respect to a wide range of filter media configurations are presented in Chapter 4. Once the optimum media pack dimensions are determined from the 2-D simulations, a

series of 3-D simulations are carried out to investigate the effects of embossed designs on the filtration performance. The findings are discussed and reported in Chapter 5. In Chapter 6, the cost analysis of the feasibility of developing an embossed media pack filter are presented. Lastly, the main findings of the research work are summarized in Chapter 7 and some further studies are suggested.

University of Malaya

CHAPTER 2: LITERATURE REVIEW

2.1 Introduction

In this chapter, the air filter performance assessments in terms of pressure drop, filtration efficiency, and dust holding capacity are reviewed in Section 2.2. Following that, the classifications of filters are presented in Section 2.3, while the different approaches of air filtration are discussed in Section 2.4. The various CFD modelling techniques utilized in simulating air filter performances are evaluated in Section 2.5. Lastly, the summary of the literature reviews is presented in Section 2.6.

2.2 Air Filter Performances

In general, the air filter performances can be classified into three different categories, such as pressure drop, filtration efficiency, and dust holding capacity. The discussions for each category are presented in Sections 2.2.1 to 2.2.3, respectively.

2.2.1 Pressure Drop

Pressure drop across an air filter usually refers to a single-value pressure loss magnitude when air passes through the filter. The pressure loss magnitude can be expressed by Equation (2-1):

$$\text{Pressure Loss} = [\text{Pressure}]_{\text{filter upstream}} - [\text{Pressure}]_{\text{filter downstream}} \quad (2 - 1)$$

Pressure drop is generally measured in terms of pascals, pounds per square inch, as well as inches of water column. It is noted that the pressure-drop measurements also imply the quantity of work needed to force /draw the air across the filter. This parameter is important, particularly for a huge system, as it governs the selection of drive fan and drive power during system design phase (Fotovati, Hosseini, Tafreshi, & Pourdeyhimi, 2011; Schousboe & Schousboe, 2017).

Knowing that pressure drop of air flow across a filter is not desired, many studies have been conducted to explore the methods to minimize the pressure losses. It is reported that both viscous loss and inertial loss are the key two factors contributing to overall pressure losses (Chen, Pui, & Liu, 1995; Tsang, 1999; Wang, Brannock, Cox, & Leslie, 2010). Therefore, balancing these two losses will aid in reducing the total pressure drop of air flow across the filter.

Furthermore, it is also found that the configurations of the filtration surface, which is exposed to the incoming air flow (and contaminant), may alter the overall pressure losses through the air filter. For instance, the implementation of pleated filtration media may cause contaminant to accumulate on the filtration surface and eventually lead to a temporal change in pressure drop.

2.2.2 Filtration Efficiency

The air filtration efficiency is typically governed by the fluid velocity to be filtered as well as the size of the contaminant to be filtered through the air filter (Mohan, Yang, & Chou, 2013; Schousboe & Schousboe, 2017; Tronville & Rivers, 2005). It is reported that when the velocity of the fluid to be filtered is reduced, the filtration efficiency increases.

On the other hand, the filtration efficiency of the air filter is a function of the contaminant's particulate size (Gras, 1994; Schousboe & Schousboe, 2017). It is important to take note the contaminant particle size range varies with respect to applications. Contaminants which are within the range of the size would be able to pass through the filter media in accordance to the streamline of air without any contact with the media surface. However, when the particle size is too big, it will not be able to penetrate through the filter media since its large inertia force has overcome the shear viscous force of air. In contrast, when the particle size is too small, the particle will flow

according to the Brownian motion and eventually be captured by the filter media through diffusion. The graphical illustrations are provided in Figure 2.1. Further descriptions can be found in Section 2.4.

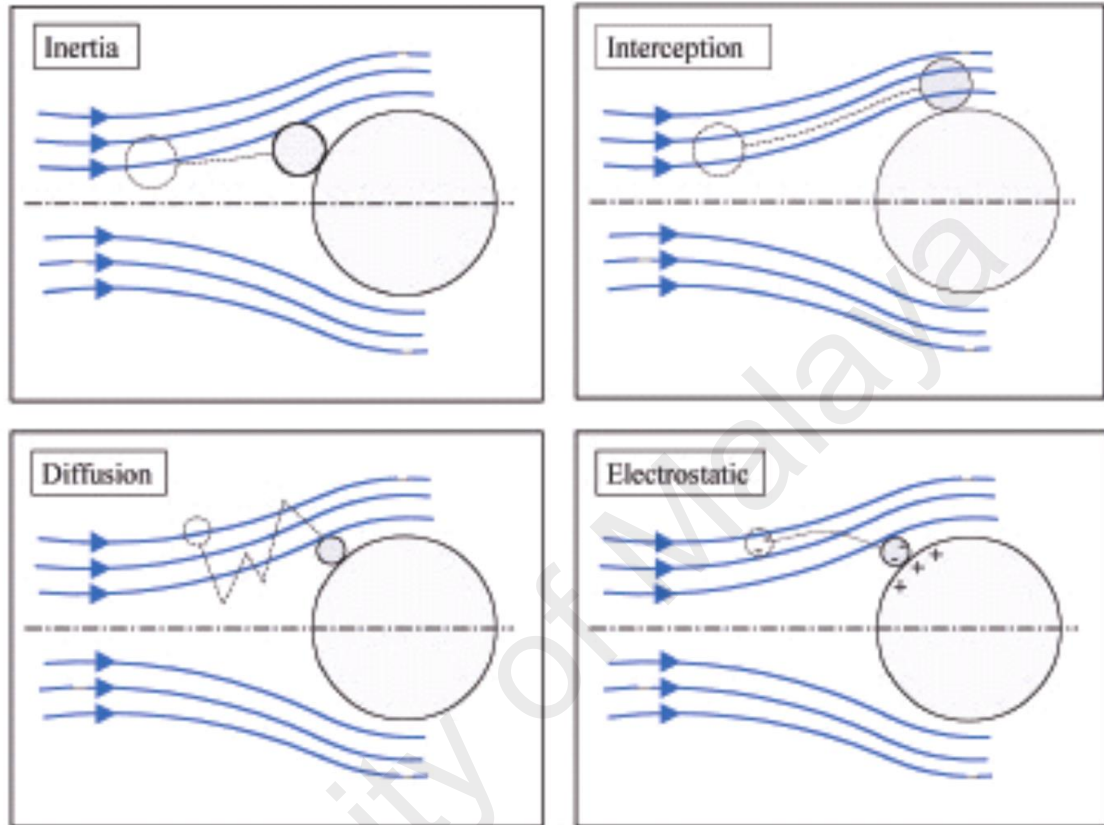


Figure 2.1: Contaminant's particle movements (GmbH, n.d.).

2.2.3 Dust Holding Capacity

Another parameter which governs the air filtration efficiency is the dust holding capacity. The dust holding capacity is defined as the amount of dust which a filter can hold at the same time as retaining the required filter's efficiency or within the rated pressure drop (Legg, 2017). It is important to highlight that the dust holding capacity does not take into the account the amount of dust which passes through the filter. One of the common test procedure is the ASHRAE 52.2. The dust holding capacity is calculated based on: (i) the amount of dust captured in a final filter downstream; (ii) the amount of dust hold in the test duct downstream and before the final filter (Hutten, 2007). Then, the

final dust holding capacity of the filter is determined by subtracting the total dust fed into the filter by the total amount of dust captured by the filter. The dust holding capacity usually has a unit of g/m^2 as it is prorated to the filter media area such that easy comparison between various filter media can be done.

The filter efficiency is correlated with the dust holding capacity, whereby the efficiency is calculated based on several measurement times over the course of the filtration test (Xu et al., 2018). This is demonstrated in Figure 2.2.

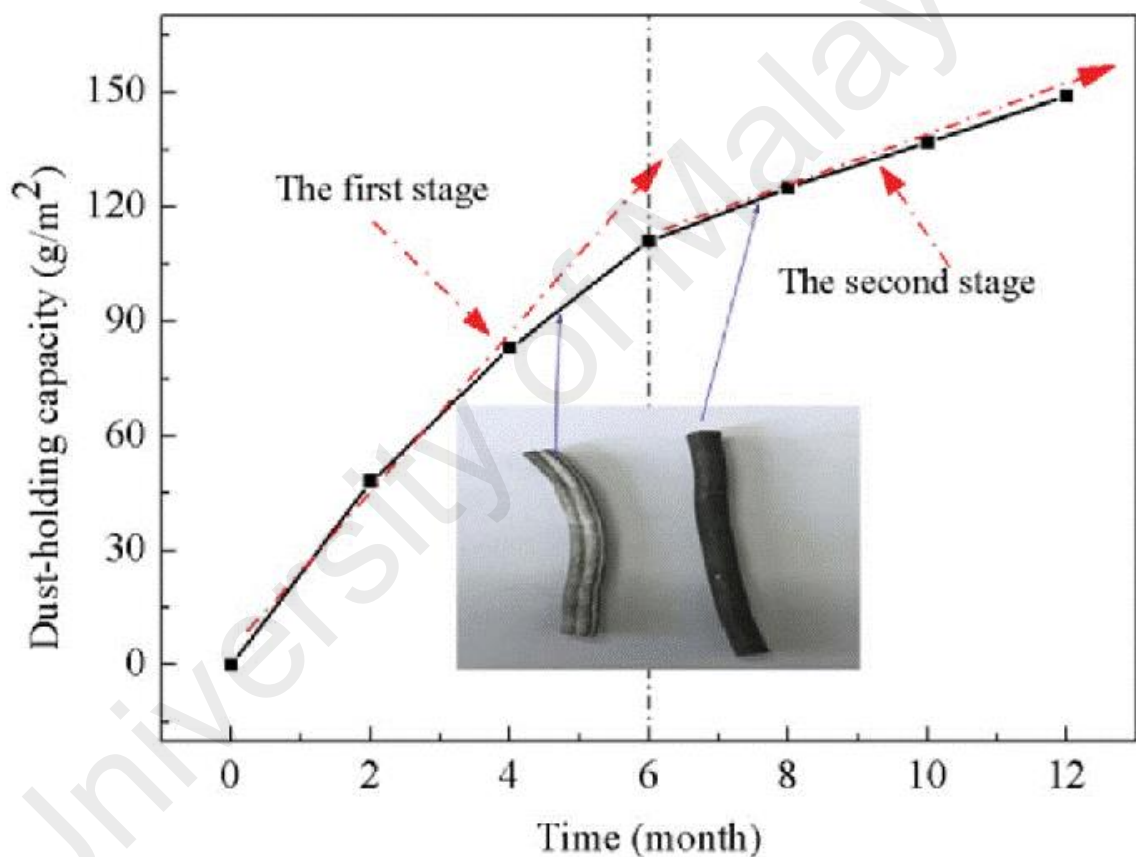


Figure 2.2: The dust holding capacity of a PTFE fibre membrane module at different times of a year (Xu et al., 2018).

On the other hand, it is reported that the dust holding capacity is not essentially associated to the pressure drop life test (Hutten, 2007). A filter with low efficiency allows more dust to pass through it and hence leads to slow pressure drop build-up. In contrast, a filter with high efficiency is able to retain more dust and subsequently leads to quicker

pressure drop build-up. As a consequence, its lifespan is shorter in comparison to a filter with relatively lower efficiency due to wear and tear.

2.3 Classifications of Filters

In general, particle filters can be categorized as coarse filter, fine filter, High-Efficiency Particulate Air (HEPA) filter, and Ultra-Low Particulate Air (ULPA) filters (Goodfellow, 2001; Liu, Rubow, & Pui, 1985; White, 2009). Some of the examples are listed in Table 2.1.

Table 2.1: Filter classifications (Purchas & Sutherland, 2002).

Type	Eurovent class	CEN EN779 class	Efficiency (%)	Measured by:	Standards
Coarse dust filter	EU1	G1	<65	Synthetic dust weight arrestance	ASHRAE 52-76 Eurovent 4/5
	EU2	G2	65<80		
	EU3	G3	80<90		
	EU4	G4	>90		
Fine dust filter	EU5	F5	40<60	Atmospheric dust spot efficiency	BS 6540 DIN 24 185 EN 779
	EU6	F6	60<80		
	EU7	F7	80<90		
	EU8	F8	90<95		
	EU9	F9	>95		
High efficient particulate air filter (HEPA)	EU10	H10	85	Sodium chloride or liquid aerosol	BS 3928 Eurovent 4/5 DIN 24 184 (DIN 24 183)
	EU11	H11	95		
	EU12	H12	99.5		
	EU13	H13	99.95		
	EU14	H14	99.995		
Ultra low penetration air filter (ULPA)	EU15	U15	99.9995	Liquid aerosol	DIN 24 184 (DIN 24 183)
	EU16	U16	99.99995		
	EU17	U17	99.999995		

The filter classifications are done based on the respective filtration efficiency which is measured with respect to a series of defined standard conditions and the system may vary from country to country owing to different measurement standards. As shown in Table 2.1, there are 17 classes of air filter according to the parallel Eurovent and European

Committee for Standardisation (CEN) classifications. Among all, there are four coarse dust filters, five fine dust filters, five HEPA filters, and three ULPA filters. Both the HEPA and ULPA filters are used to trap submicrometre particles.

The efficiency ratings provided in the table are based on the actual filters in an efficient filtration system. Nonetheless, in practical, the efficiency of the air filter will also be influenced by the collective effect of the filter media used, as well as fluid flow which has bypassed the filter system through gaps/cracks (Purchas & Sutherland, 2002). While leakages are hard to be prevented in realistic, an actual filter will generally possess a lower efficiency as compared to the rating given in Table 2.1.

2.4 Common Air Filtration Methods

There are four common types of air filtration methods such as barrier filtration, inertial separation, chemical adsorption, and catalyst. Details of each method are depicted in Sections 2.4.1 to 2.4.4, respectively.

2.4.1 Barrier Filtration

Barrier filtration, as its name suggested, usually applies the concept of physical barrier to remove the unwanted compounds of fluid passing through it. Surface filtration as well as depth filtration are the common types of barrier filtration approaches.

First of all, the surface filtration uses a layer of net-like structure to filter the contaminant whereby the particles will be captured in the net and build upon the surface. It is important to highlight that increasing the layers of the net in series will not enhance the filter's performance as the performance is merely determined by the pore size of the filter media. The schematic diagram of surface filtration is presented in Figure 2.3.

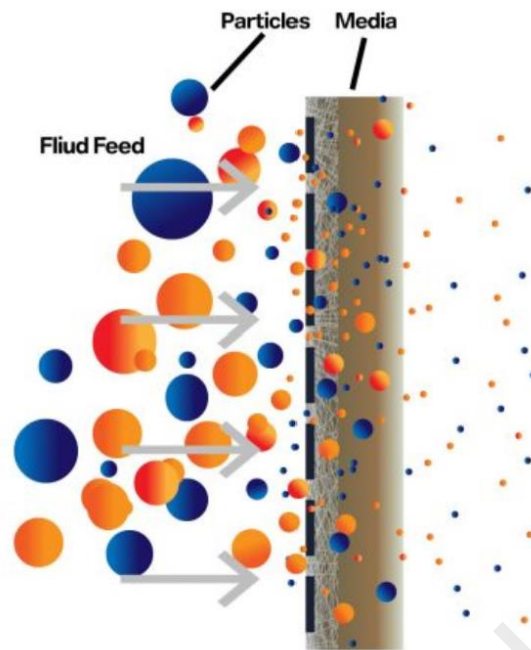


Figure 2.3: Schematic diagram of surface filtration (Gopani, n.d.).

The second type of barrier filtration is the depth filtration. Unlike the surface filtration, the performance of the depth filter varies according to time. The schematic diagram of depth filtration is presented in Figure 2.4.

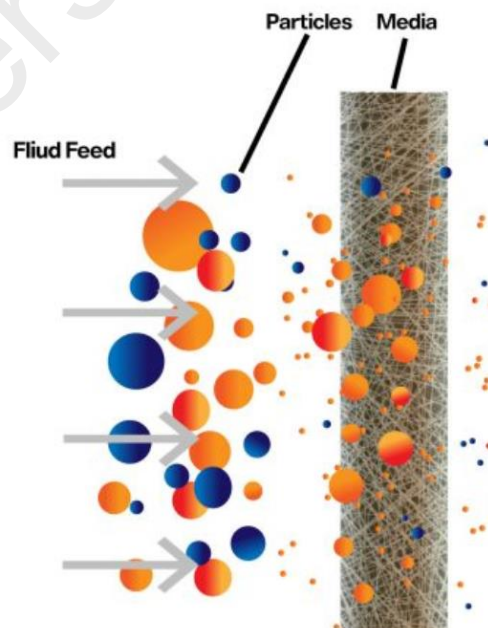


Figure 2.4: Depth filtration (Gopani, n.d.).

Direct interception, inertial impaction, and diffusion are the three mechanisms of depth filtration. Direct interception occurs when the contaminant particle that flows along the fluid streamline contacts with a fiber in the depth filtration media (see Figure 2.1). It is presumed that the contaminant will stick to the fiber when it travels through a path which is less than one particle radius away from the filter media's fiber (Schousboe & Schousboe, 2017).

On the other hand, as shown in Figure 2.1, inertial impaction takes place when the inertia of the contaminant particle is sufficiently high such that the drag force exerted by the air flow on the particle is not adequate to change the particle's trajectory, and eventually the contaminant particle is brought to contact with the fiber.

Lastly, diffusion mechanism involves contaminant particles which have very small particle diameter and these particles are unable to be captured using the aforementioned two mechanisms. The contaminant particles rapidly reach thermal equilibrium with the surrounding gas and eventually undergoes Brownian motion (Gras, 1994). Under such circumstances, the smaller contaminant particles will travel at greater average velocity as compared to the larger particles. The particles are captured through diffusional deposition in which it is a function of the magnitude of the diffusional motion as well as the fluid's convective motion around the media fiber.

2.4.2 Inertial Separation

Inertial separation approach involves dividing the inbound air flow into different paths and changing the filter geometry such that the contaminant particles could not follow the stream of air across the filter. The system is termed as the inertial particle separator. The schematic diagram of the inertial particle separator is provided in Figure 2.5.

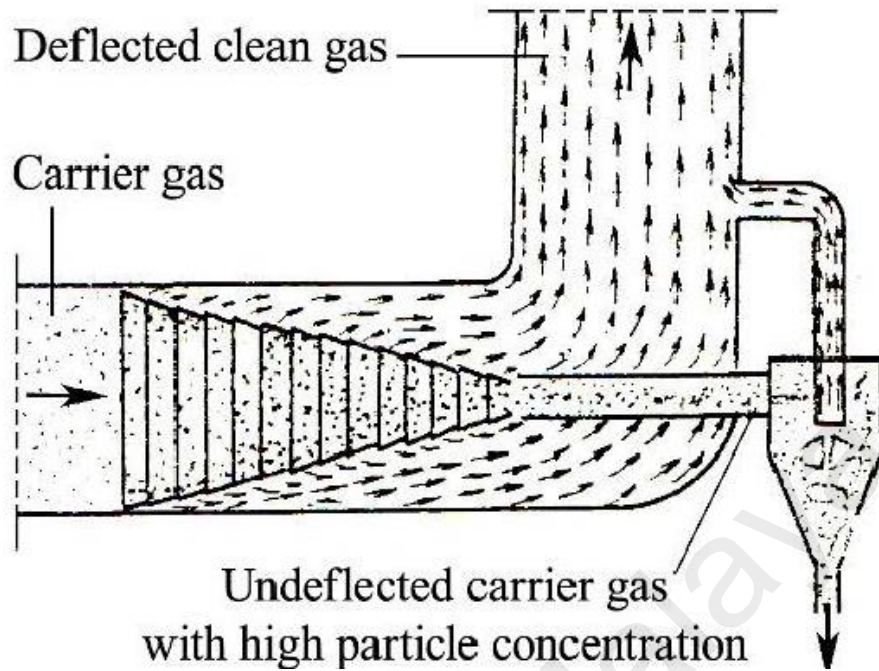


Figure 2.5: Schematic diagram of inertial separation (Domnița, Bacoțiu, Hoțupan, Popovici, & Kapalo, 2014).

The main benefits of utilizing the inertial separator system are: (i) The rather steady state behavior of the system; (ii) minimal maintenance is required as it involves very little moving parts. Nevertheless, one of the disadvantages of the system is that a driven source is necessary to scavenge the particle-overloaded air.

2.4.3 Chemical Adsorption

Chemical adsorption filter is often applied to eliminate volatile organic compounds. Unlike the barrier filtration method, chemical adsorption approach utilizes solid surface which is tuned to attract and then adsorb unwanted chemical compounds. It is noted that the efficiency of a chemical adsorber reduces with increasing contaminant adsorbed. Therefore, it is often designed to be a single-use item only (Bull & Roux, 2010). An example of a chemical adsorber is shown in Figure 2.6.



Figure 2.6: chemical adsorber.

2.4.4 Catalysts

Catalyst filter requires heat to perform the chemical reaction for filtration purpose and this type of filter is generally found in aerospace applications (Bull & Roux, 2010; Van der Smissen, 1987). One of the popular catalyst filters is the ozone catalyst which is installed in the aircraft to oxidize the O_3 molecules in order to prevent them from damaging the onboard system at high altitudes. The system contains a honeycomb substrate material which is usually coated with special chemical compounds for specific applications. An example of ozone catalyst filter is shown in Figure 2.7.



Figure 2.7: Ozone catalyst filter.

2.5 CFD Modelling Techniques

According to the research study conducted by Tronville and Sala (2003), the performance of a prototyped mini-pleated air filters is improved through the implementation of an empirical correlation, while the pressure drop across the filter is successfully minimized. Both 2-D and 3-D CFD analysis are conducted using various types of filter media to examine the fluid flow field in the filter system. Their findings show that the pressure drop across the filter is a function of the number of pleats per unit length.

A series of CFD analysis are conducted by Del Fabbro et al. (2002) to study the relations of pressure drop through pleater filters (HEPA and low efficiency particulate) with types of filter media, pleating geometries as well as air flow parameters. The results are compared against the experimental measurements. Their research findings show that a more consistent and well-distributed air flow takes place over the pleated filter surface. Besides, the effects of geometric characteristics on the initial pressure drop across LE filter is greater than that of HEPA filter.

Furthermore, it is noted that pleated filters which integrate an electrostatic precipitator are commonly utilized in capturing particle contaminants in enclosed regions (Feng, Long, & Chen, 2014). In their study, CFD analysis are performed to assess the various types of turbulence model in determining the pressure drop and transitional flows across pleated filters with and without the presence of an electrostatic precipitator. As compared to the experimental data, the Detached Eddy Simulation (DES) and the v2f models are suggested to be applied in optimizing the pleated filter system design.

In the research work of Yue et al. (2016), the 3-D random structures of fibrous filters are generated to examine the filtration process within the fibrous filters. The CFD approach coupled with the discrete element method (DEM) is used to simulate the

interactions between contaminant particles, filter fibers and fluid. Calculations on the filtration efficiency and pressure drop across the filter are performed and the simulation results are validated in CFD-DEM with the use of the semi-analytical models. Their findings show that the filtration performance is dependent on the particle diameter, fiber diameter, as well as fluid velocity.

In addition, Qian et al. (2014) have developed 3-D fibrous media models to study the particle deposition morphology as well as the evolutions of the instantaneous pressure drop and efficiency using the CFD-DEM approach. The characteristics of the gas-solid flow in fibrous media exposed to particle loading are simulated and validated against the data from literature. Their simulation results indicate that the filtration performance of the fibrous media is dependent on the porosity of fibrous media, face velocity and particle size.

A rectangular filter with U-shaped pleats is employed by Schousboe (2017) to investigate the effects of changing filter media geometries on the filtration performance using CFD approach. The geometry parameters include pleat density, pleat height, as well as media thickness. From the simulation studies, it is found that the maximum local velocity exists at the tip of the upstream pleat form. Additionally, when the pleat density and pleat height are increased, the deviation in the maximum local velocity is increased as well.

Filter media with pleated shape is always favorable as the design is able to reduce pressure drop across filter as well as to increase the filtration area. In view of this, theoretical, experimental and simulation investigations are conducted to investigate the impacts of pleat number and pleat height on the pressure drop of fluid flow across filter (Fu, Fu, & Xu, 2014). Based on the results obtained, it is found that when pleat spacing

is reduced and when pleats height is increased, the filtration area is increased and subsequently the overall pressure drop across the filters is reduced.

2.6 Chapter Conclusions

Based on the literature reviews conducted in this study, it is concluded that pleat density, pleat height, and pleat depth play an important role in determining the filtration performance of the air filter. Therefore, these parameters are selected in this CFD modelling study and the results are presented in Chapters 4 and 5.

University of Malaya

CHAPTER 3: RESEARCH METHODOLOGY

3.1 Introduction

In this chapter, the research methodology employed to carry out the project is described in Section 3.2, followed by the presentation of the project timelines in Section 3.3. Next, the numerical models and the computational grid used in the CFD simulations are described in Section 3.4. Finally, the chapter conclusions are presented in Section 3.5.

3.2 Project Flow

At the beginning phase of the project, a comprehensive literature review is performed to evaluate the various CFD modelling techniques applied in air flow simulations across filter media pack. Besides, the specifications of the filter used in this research study are examined and the relevant information will be used in the CFD model formulations in the next phase of work. A 2-D computational mesh is also constructed for the numerical simulations and grid independency test is carry out.

The second phase of the project deals with 2-D simulations of various configurations of filter media. First of all, the computed pressure difference across a flat filter media is compared with the experimental data for validation purpose. The CFD numerical models applied here are described in Section 3.4. Upon successful model validations, the same numerical settings are applied to carry out a series of parametric studies using different filter media configurations such as installation angles, pleat heights, and pleat densities. As a consequence, the optimum media pack dimensions are determined.

The last phase of the project deals with the 3-D modelling od standard media pack and embossed media pack. The effects of the embossment on the filter media performance in terms of initial resistance, dust holding capacity, and cost are evaluated here.

The research flow chart of this project is demonstrated in Figure 3.1.

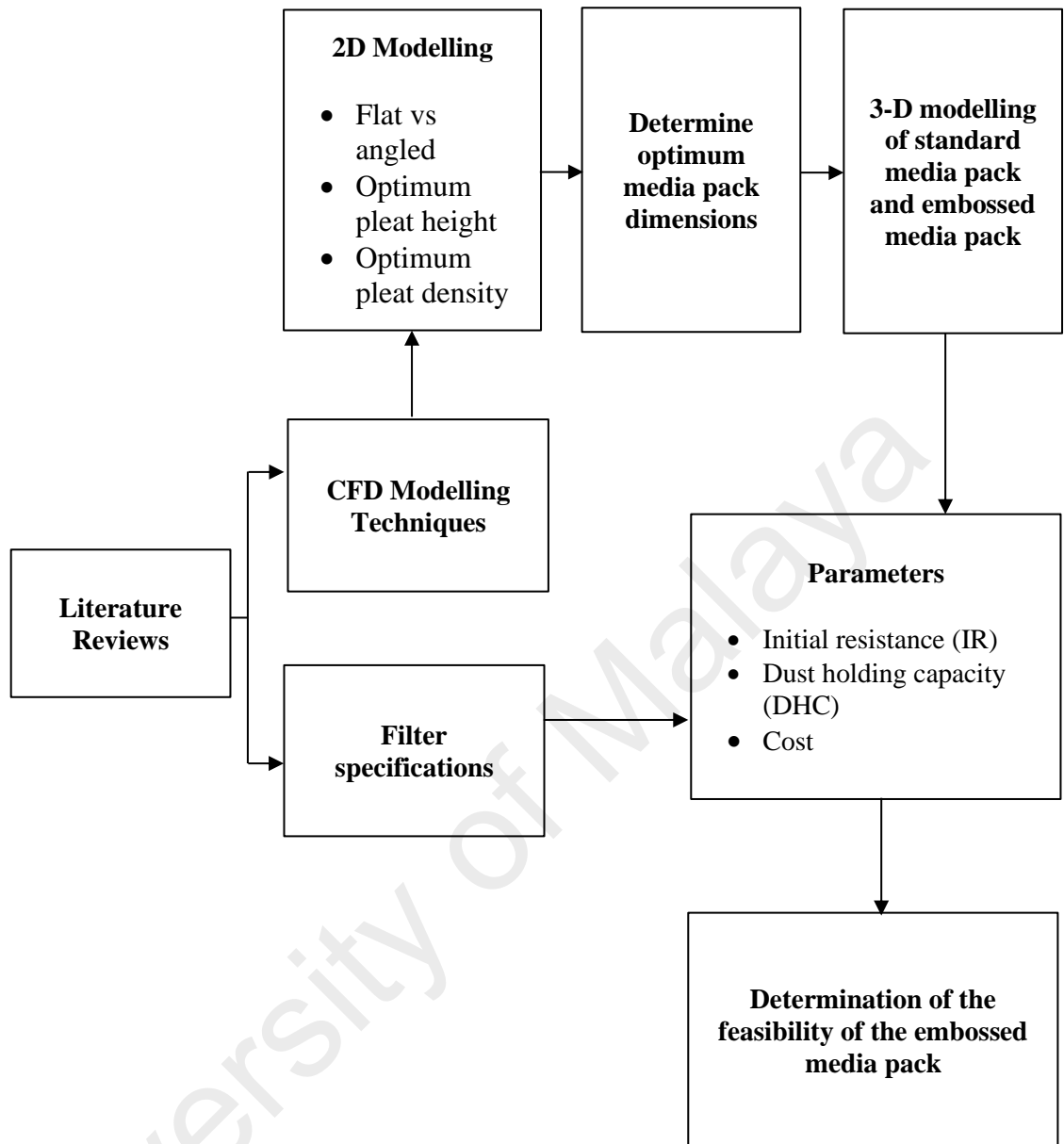


Figure 3.1: Research flow chart of project.

3.3 Project Timeline

Both the planned and actual project schedules to accomplish the project are presented in Table 3.1. The duration taken to complete the research is approximately nine months, which can be divided into three phases of work. Each phase of work requires around three months to complete.

Table 3.1: Project schedule.

Phase	Activities	Duration (Months)	Month									
			1	2	3	4	5	6	7	8	9	
1	Literature review	3	Planned	Actual								
	Mesh generation, numerical model formulation			Planned	Actual							
2	Model validations	3				Planned	Actual					
	Parametric studies in 2-D simulations						Planned	Actual				
3	3-D simulations	3							Planned	Actual		
	Thesis writing										Planned	Actual

 Planned schedule
  Actual schedule

According to Table 3.1, The first phase of the project is completed in compliance with the proposed timelines. For the second phase of the project, the actual CFD model validation process has taken shorter time to complete as compared to the projected timeline, while additional time is required to finish the parametric studies in 2-D simulations. In spite of these, the second phase of work is completed on time. Lastly, the 3-D simulations in Phase 3 of the project are completed two weeks earlier than the planned schedule and more time is allocated for report writing. The overall project is delivered timely.

3.4 CFD Configurations

The descriptions of the CFD models used are provided in Section 3.4.1 together with their corresponding governing equations. On the other hand, the details of the computational grid applied in the simulations are depicted in Section 3.4.2.

3.4.1 CFD Models

Viscous model – Shear-Stress Transport (SST) k - ω Model

For all the 2-D and 3-D simulation studies, SST k - ω model (Ferziger & Perić, 2002; Fluent, 2015; Roache, 1998) is applied to compute the turbulence behaviors of the air flow across filter media pack. The turbulence kinetic energy, k , and the turbulence specific dissipation rate, ω , are defined by Equations (3-1) and (3-2), respectively.

$$\frac{\delta}{\delta t}(\rho k) + \frac{\delta}{\delta x_i}(\rho k u_i) = \frac{\delta}{\delta x_j} \left(\Gamma_k \frac{\delta k}{\delta x_j} \right) + \widetilde{G}_k - Y_k + S_k \quad (3-1)$$

$$\frac{\delta}{\delta t}(\rho \omega) + \frac{\delta}{\delta x_i}(\rho \omega u_i) = \frac{\delta}{\delta x_j} \left(\Gamma_\omega \frac{\delta \omega}{\delta x_j} \right) + \widetilde{G}_\omega - Y_\omega + D_\omega + S_\omega \quad (3-2)$$

Where \widetilde{G}_k and \widetilde{G}_ω are the generation of turbulence kinetic energy and turbulence specific dissipation rate due to mean velocity gradients u , respectively. Note that Γ_k and Γ_ω refer to the effective diffusivity of turbulence kinetic energy and turbulence specific dissipation rate, respectively. Besides, Y_k and Y_ω refers to the dissipation of kinetic energy and specific dissipation rate as a result of turbulence. D_ω refers to the cross-diffusion term while both S_k and S_ω are the user-defined source terms.

Porous Media Model

An empirically defined flow resistance is integrated in the porous media model to model the user-defined porous region (Fluent, 2015; Tu, Yeoh, & Liu, 2018). A momentum source term is incorporated in the governing equations for momentum calculations which covers a viscous loss term and an inertial loss term. This is described by Equation (3-3) as follows:

$$S_i = - \left(\frac{\mu}{\alpha} v_i + C_2 \frac{1}{2} \rho |v| v_i \right) \quad (3-3)$$

Where S_i represents the source terms for the i^{th} momentum equation, μ represents the viscosity, α represents the permeability, ρ represents the density, $|v|$ represents the velocity magnitude, and C_2 represents the inertial resistance factor.

3.4.2 Computational Meshes

The computational meshes for both 2-D and 3-D simulations are depicted in Figures 3.2 and 3.3, respectively.

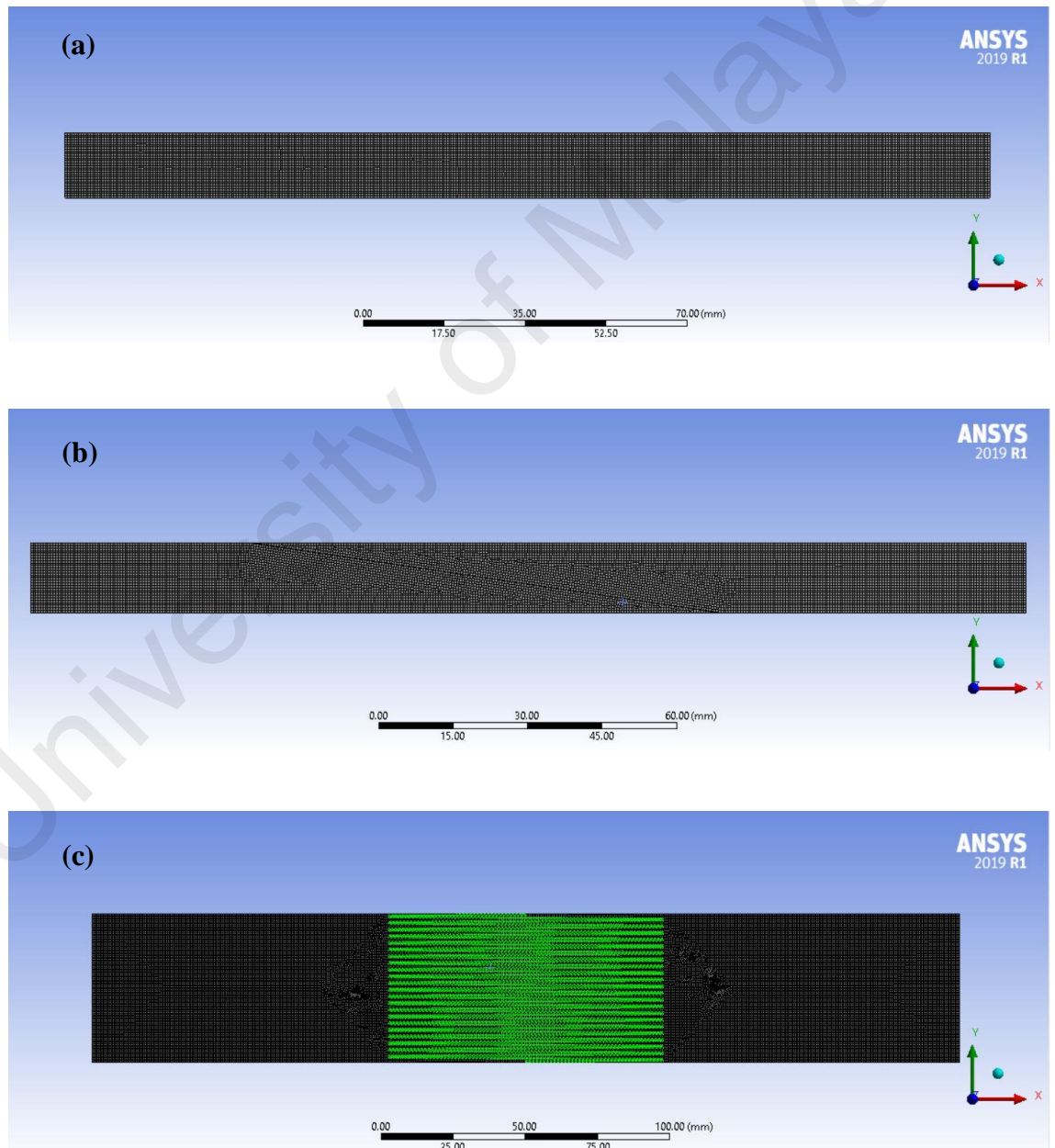
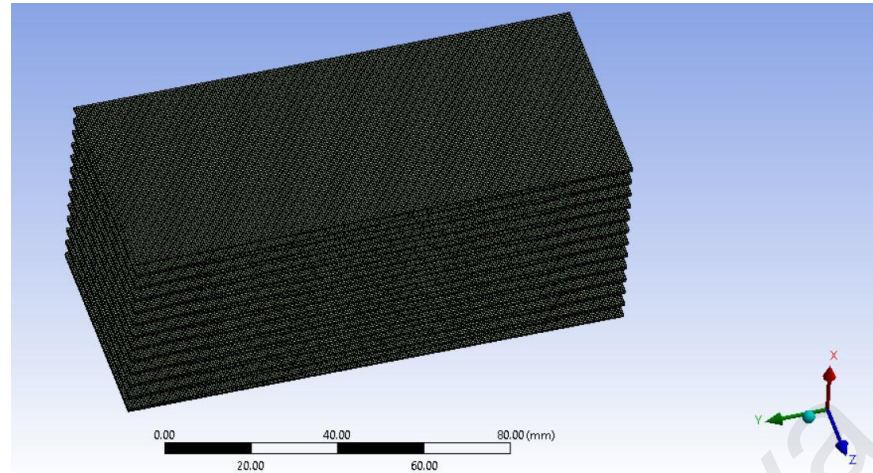
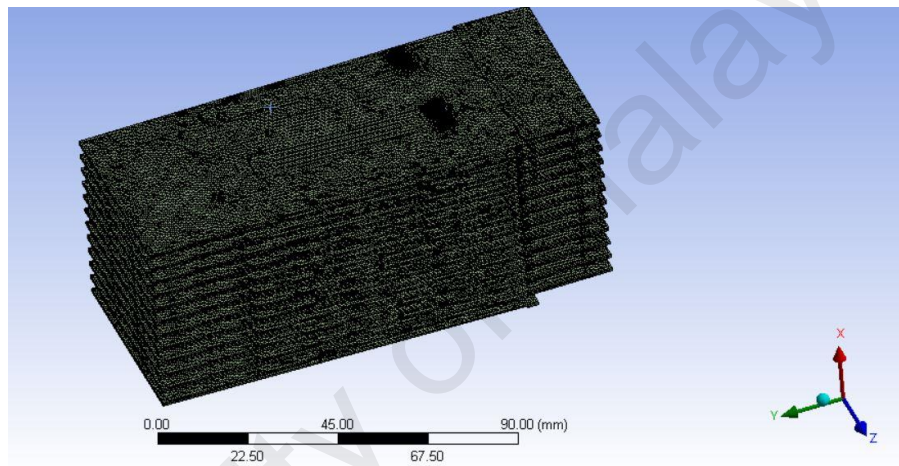


Figure 3.2: 2-D computational grids with (a) straight media pack, (b) angled media pack, and (c) multiple pleats.

(a)



(b)



(c)

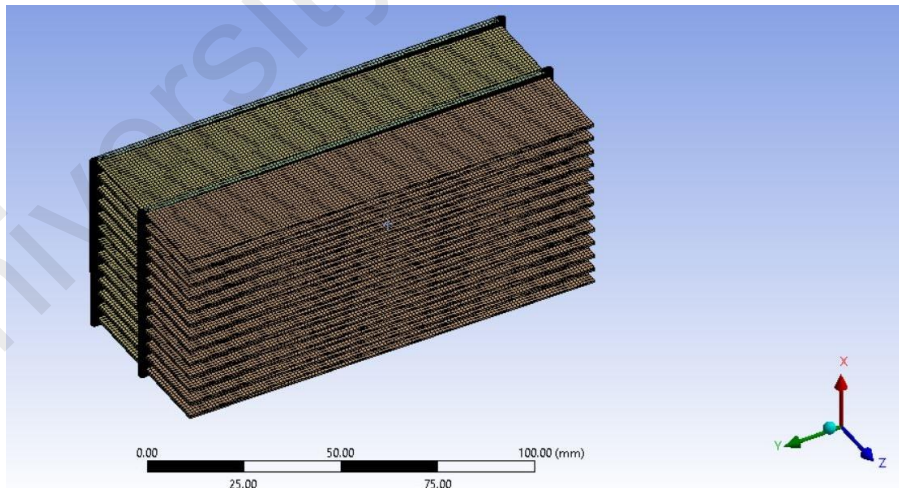


Figure 3.3: 3-D computational grids for pleated filter media model (a) without emboss, (b) with emboss, and (c) with hot melt adhesive layers.

All the computational meshes are well validated through grid independency test with respect to pressure difference across the filter media pack. Grid size of 0.1 mm is applied

for all the computational meshes. It is noted that the model predictions are consistent when smaller grid sizes are applied. Therefore, grid size of 0.5 mm is sufficient for the simulation studies in order to minimize the computational time and yet maintain the model accuracy. Besides, quadrilateral mesh type is chosen for 2-D simulations, while hexahedral mesh type is chosen for 3-D simulations since they both are space efficient and yet highly accurate. The details of the computational grids for various simulation settings are listed in Table 3.2.

Table 3.2: Details of the computational grids for both 2-D and 3-D simulation studies.

Settings	Number of elements
2-D model with straight media pack	11,200
2-D model with angled media pack ¹	11,398 – 12,102
2-D model with multiple pleats ²	61,865 – 64,491
3-D model ³	5,800,396 – 6,030,678

¹ Number of elements depends on the angles of the media pack (5.5° to 11.5°)

² Number of elements depends on the number of pleats of the media pack (3 pleats to 11 pleats)

³ Number of elements depends on the design (i.e. with or without emboss and hot melt adhesive layers)

3.5 Chapter Conclusions

In this chapter, the methodology used to conduct the research study are discussed in detail. Following that, the planned and actual project schedules are presented and discussed. Lastly, the CFD models applied in the numerical simulations are described, along with the associated governing equations. On top of that, the numerical mesh constructed for the simulations is presented and grid independency test is performed. To sum up, the entire project is delivered on time.

CHAPTER 4: 2-D CFD SIMULATIONS

4.1 Introduction

First of all, model validations are carried out with respect to experimental data and the results are reported in Section 4.2. Subsequently, parametric studies are performed with respect to variations in height, angle, number of pleats, and pleat height of the filter media pack. Discussions for each parameters are presented in Section 4.3. Finally, the main research findings of this chapter are depicted in Section 4.4.

4.2 Model Validations

The CFD modelling technique used to model the filter medium is the porous medium model. The parameters to input to the ANSYS software to model a porous medium was calculated using Equation 3-3. A simple model of a flat sheet of filter media in the centre of a duct was simulated in a 2D environment. The thickness of the filter media was set as 0.5mm, as this is a commonly found thickness for filter media. The results of the simulation are presented in Figure 4.1.

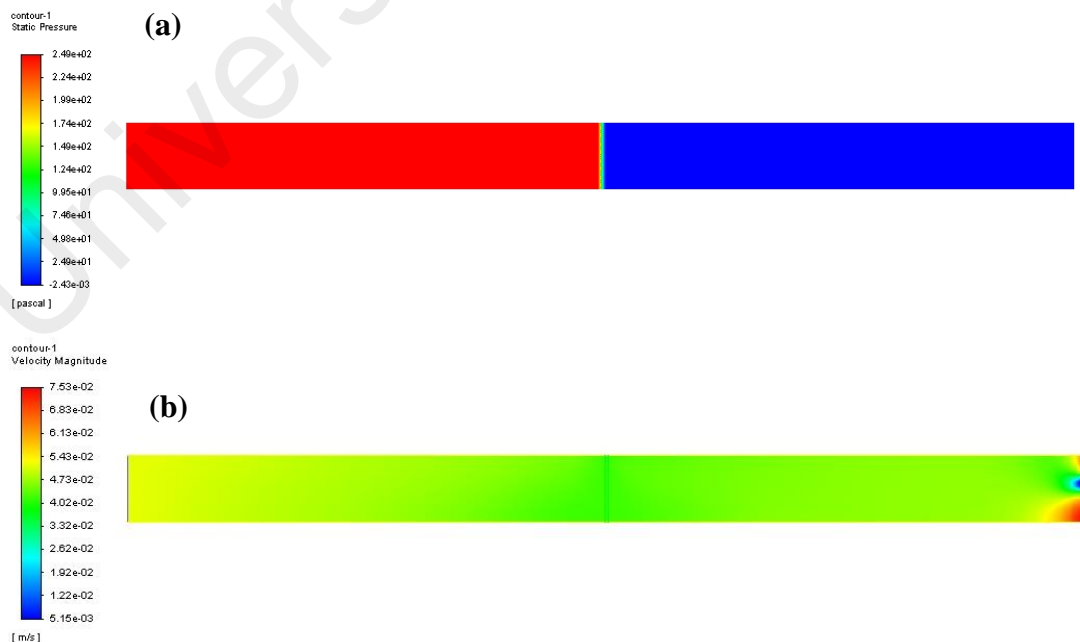


Figure 4.1: (a) Pressure drop and (b) velocity vector of the air flow across a straight filter media sheet.

From Figure 4.1, the pressure at the upstream of the filter media is higher than the pressure at the downstream. The differences of these two pressures are the pressure drop across the filter media. This pressure drop is then compared with a typical Data Sheet of a filter media manufacturer and was found to be consistent with the manufacturer's data. This validates that the input parameters of the model is accurate and the model is a good representation of the physical filter media. Besides that, the velocity vector across the filter media also shows an expected trend whereby the velocity decreases as the air flow passes through the filter media. Therefore, the input parameters of the model is used for further parametric studies.

4.3 Parametric Studies

In this section, parametric studies are performed with respect to variations in height, angle, pleat density, and pleat depth of the filter media pack. The results for each parameter are presented in Sections 4.3.1 to 4.3.4, respectively.

4.3.1 Variation in the Height of the Filter Media

The first parametric study that was carried out is to investigate the effects of the media height. The height of the media was increased from 70mm to 146mm, as shown in Figure 4.2, whilst keeping the flow rate across the filter media as a constant. This is done by decreasing the inlet velocity proportionally to the increase of the filter height. From Figure 4.3, the pressure drop across the filter media decreases as the filter height is increased. This is due to there is more space available for the air to flow across the filter media. In application, this would mean that an air filter with larger surface area will have lower resistance when subjected to a constant air flow. However, it is not practical to design an air filter that is indefinitely large. Hence, air filter manufacturers would fold the media into a pleated media pack to increase the amount of space available for the air flow.

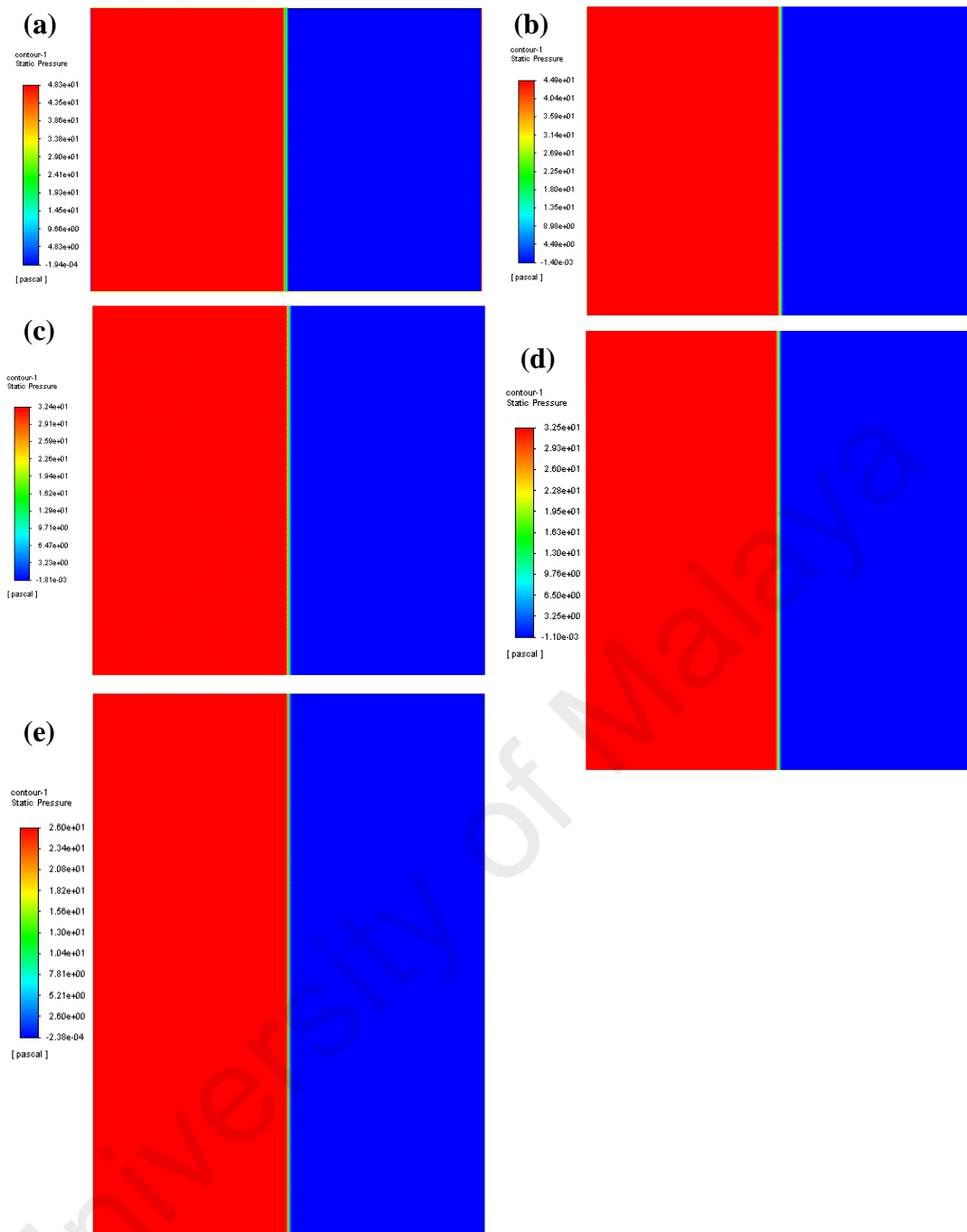


Figure 4.2: Pressure drop across straight filter media packs with height of (a) 70 mm, (b) 80 mm, (c) 94 mm, (d) 114 mm, and (e) 146 mm.

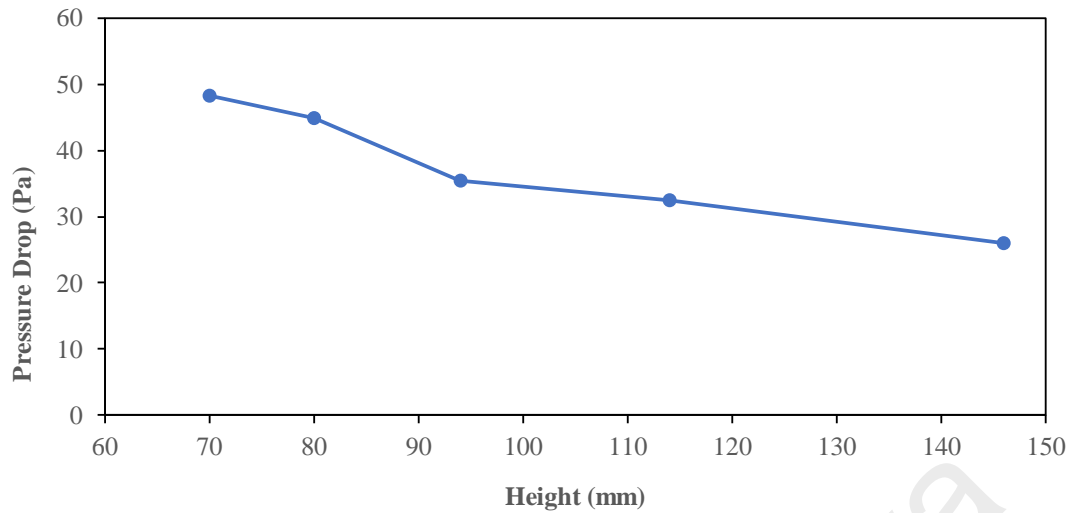


Figure 4.3: Graph of pressure drop predictions against heights of filter media packs.

4.3.2 Variation in the Angle of the Filter Media

When the filter media are folded into a filter media pack, the filter media will no longer be perpendicular to the air flow direction. To decrease the pressure drop, the filter media must be tilted at an angle. In other words, to pack more filter media into the same confined cross section area, the filter media are required to be tilted more. This effect was investigated by keeping the height of the duct constant and varying the angle of the filter media, as shown in Figure 4.4. The tilt angle is defined as the angle between the filter media and the duct wall. From Figure Figure 4.5, it is observed that the velocity vector across the media tends to be normal to the media. This demonstrates the effect of tilting the media is similar to increasing the filter media height, as shown in Figure 4.2. Furthermore, Figure 4.6 shows that the pressure drop decreases as the tilt angle decreases. However, at 5.5° and 7.0° , the pressure drop is less significant. This is due to the inertial resistance of the air flow is increasingly dominant as the air is required to flow farther downstream. Therefore, there is always an optimum angle for the filter media.

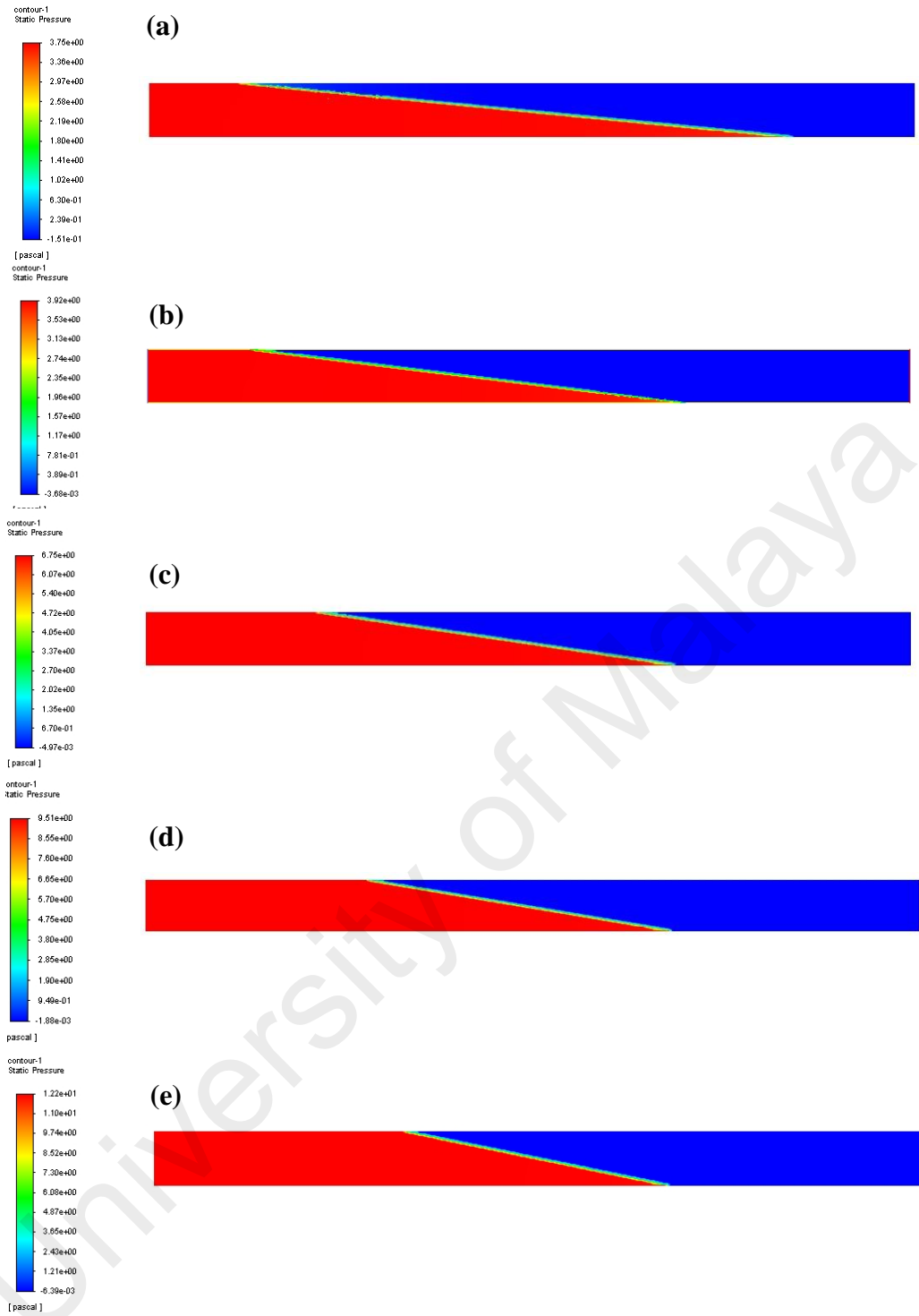


Figure 4.4: Pressure drop across filter media packs with installation angle of (a) 5.5°, (b) 7°, (c) 8.5°, (d) 10°, and (e) 11.5°.

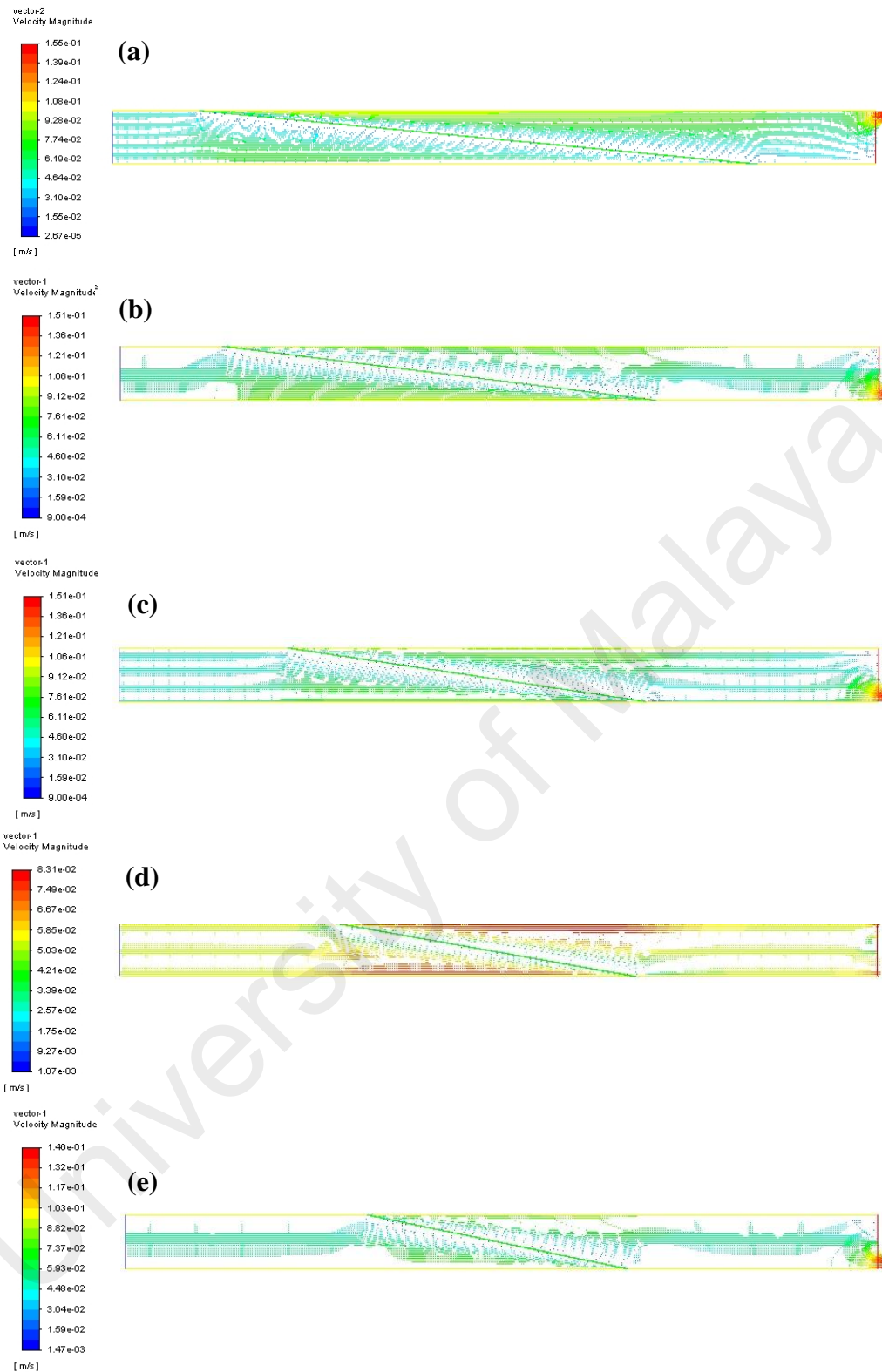


Figure 4.5: Velocity vectors of the air flow across filter media pack with installation angle of (a) 5.5°, (b) 7°, (c) 8.5°, (d) 10°, and (e) 11.5°.

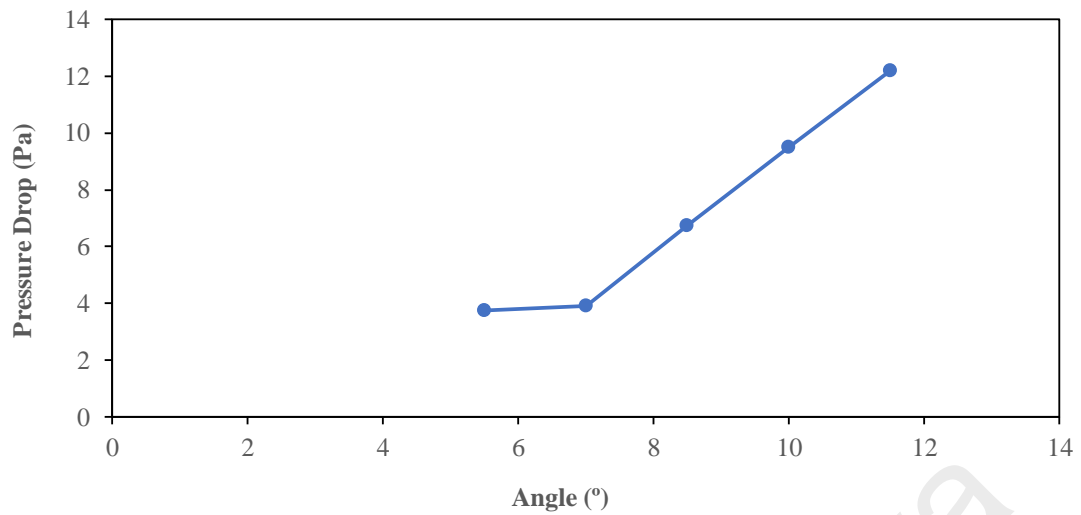


Figure 4.6: Graph of pressure drop predictions against installation angles of filter media packs.

4.3.3 Variation in the Pleat Density of the Filter Media Pack

As the angle of the tilted media has a threshold whereby the pressure drop do not decrease significantly anymore, the next alternative to further increase the space available for the air flow is to fold the media into a media pack, as previously mentioned in Section 4.3.1. To increase the amount of space, more number of pleats are added to form the media pack. Consequently, this would also result to the filter media having a smaller angle, as described in Section 4.3.3.

To normalize the dimensions of a media pack, the number of pleats is represented by the pleat density which have a unit measurement of Pleat Per Inch (PPI). To investigate the effect of the pleat density, the model was simulated at constant inlet air velocity, media pack depth and duct height, whilst the pleat density was increased from 3 PPI to 11 PPI, as shown in Figure 4.7. The velocity vector of the model is presented in Figure 4.8, which shows that the flow is more evenly distributed from 6 PPI to 8 PPI. Besides that, the colour contour also indicates a higher air velocity at this region of 6 PPI to 8PPI.

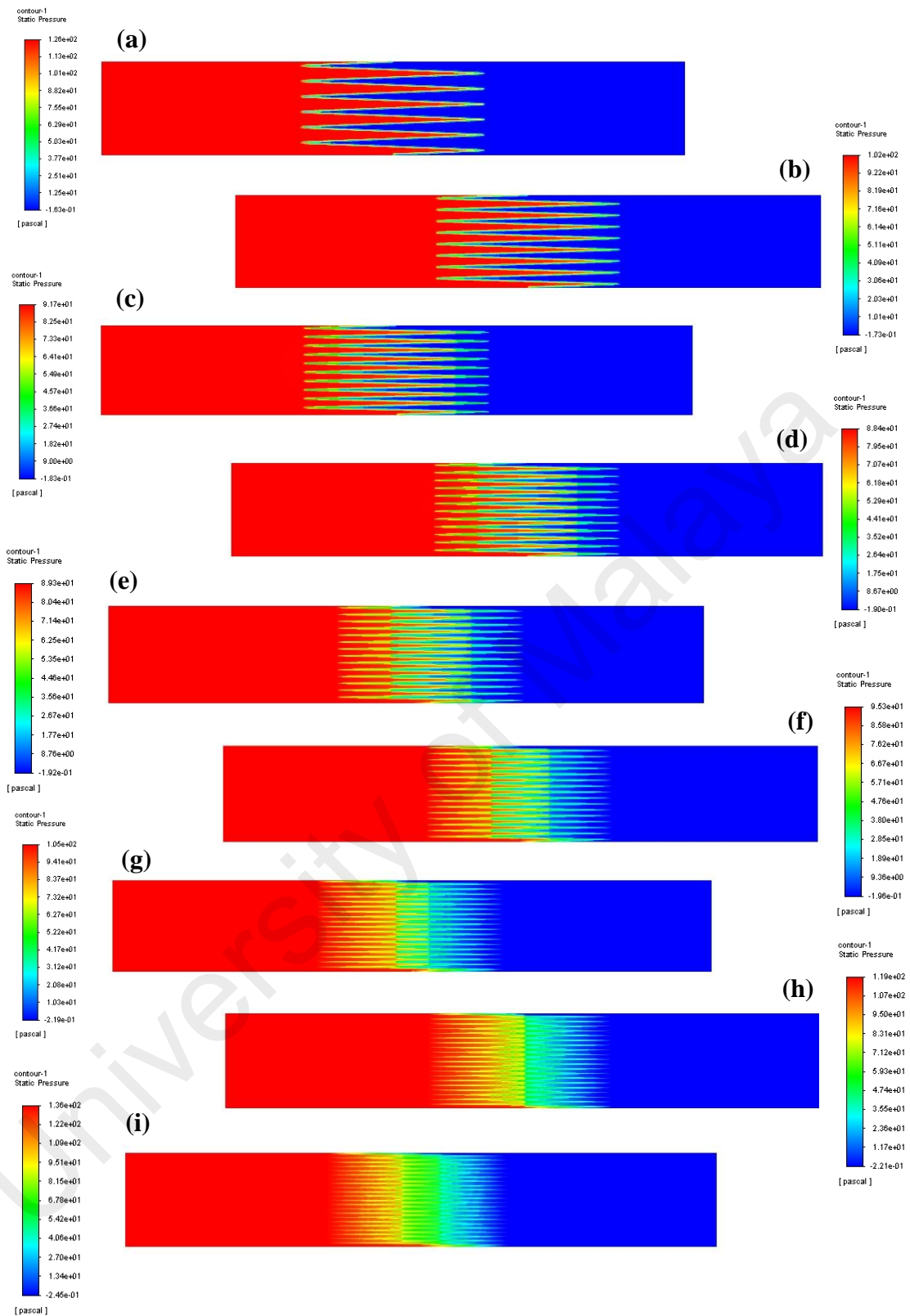


Figure 4.7: Pressure drop across filter media packs with pleat density of (a) 3, (b) 4, (c) 5, (d) 6, (e) 7, (f) 8, (g) 9, (h) 10, and (i) 11 pleats/inch.

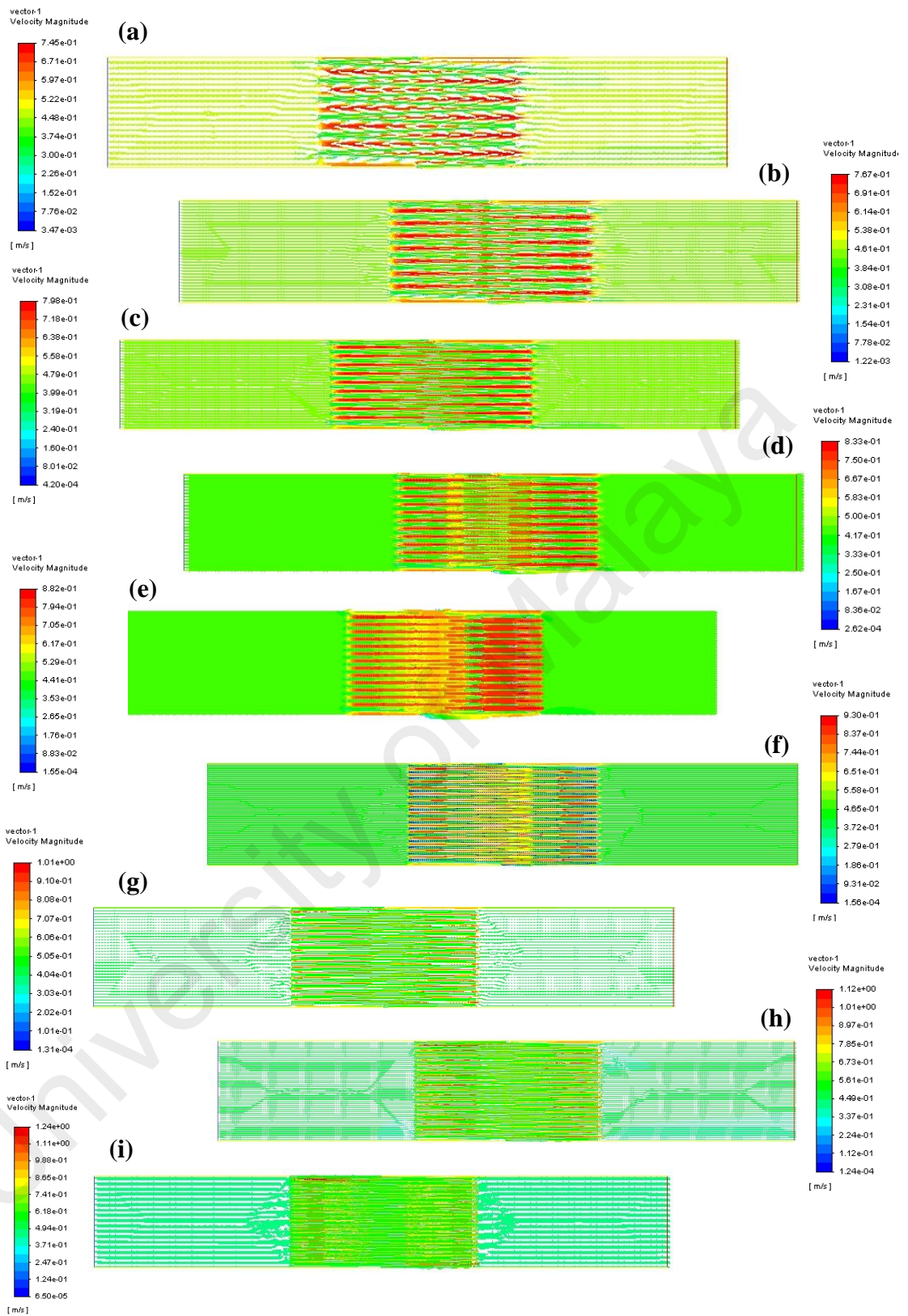


Figure 4.8: Velocity vectors of the air flow across filter media pack with pleat density of (a) 3, (b) 4, (c) 5, (d) 6, (e) 7, (f) 8, (g) 9, (h) 10, and (i) 11 pleats/inch.

In addition to that, the pressure drop across the media pack are plotted against the Pleat Density in Figure 4.9, which shows that there is an optimum at 6 PPI. This indicates that at 6 PPI, the number of pleats is optimum to encourage the air flow across the media pack. At lower Pleat Density, there is lesser amount of space available for the air flow. On the other hand, at high Pleat Density, the media pack is too compact and resembles a block of filter media resisting the air flow.

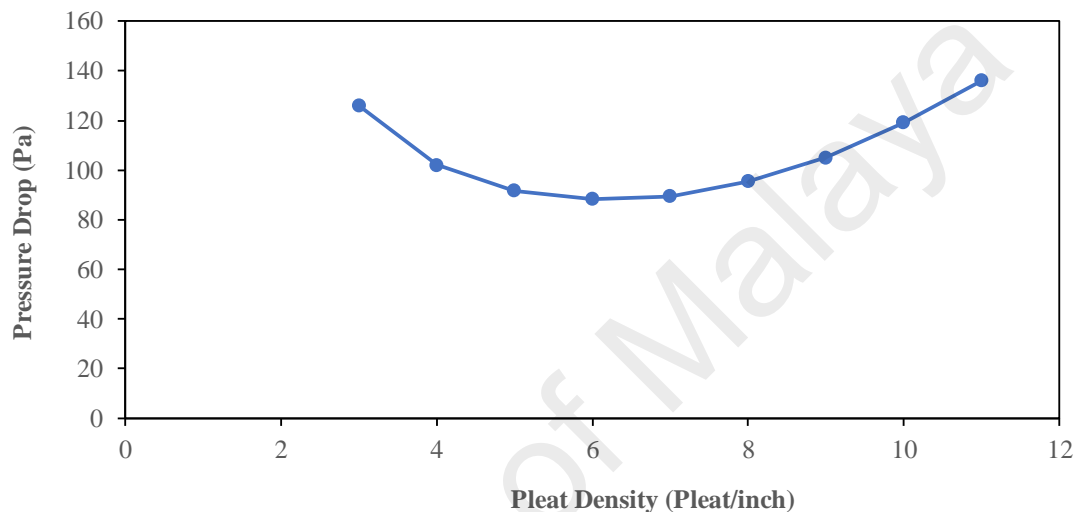


Figure 4.9: Graph of pressure drop predictions against pleat density of filter media packs.

4.3.4 Variation in the Pleat Depth of the Filter Media Pack

Using the optimum Pleat Density, the effects of the Pleat Depth of the Filter Media Pack was investigated. The Pleat Depth was varied from 12mm to 150mm with the pleat density fixed at 6 PPI, as shown in Figure 4.10. The velocity vector of the models are plotted in Figure 4.11, and an optimum can be observed at the region of 95mm to 135mm. By further plotting the Pressure Drop against the Pleat Depth in Figure 4.12, the minimum Pressure Drop occurred at the Pleat Depth of 120mm. Furthermore, beyond this optimum point, there is no significant changes of the Pressure Drop as the Pleat Depth continues to increase. This phenomenon is similar to the investigation in Section 4.3.2, whereby there

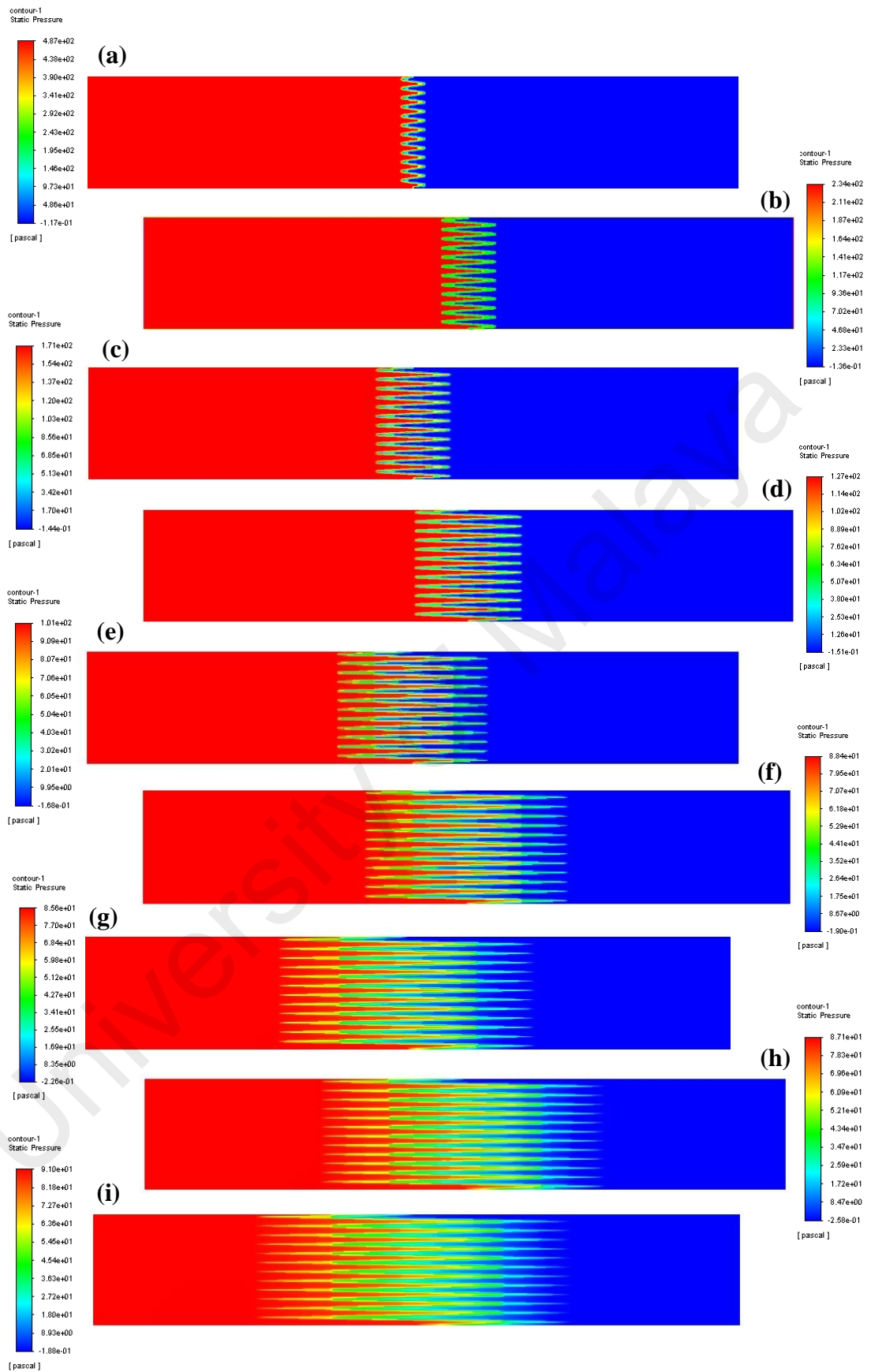


Figure 4.10: Pressure drop across filter media packs with pleat depth of (a) 12 mm, (b) 25 mm, (c) 35 mm, (d) 50 mm, (e) 70 mm, (f) 95 mm, (g) 120 mm, (h) 135 mm, and (i) 150 mm.

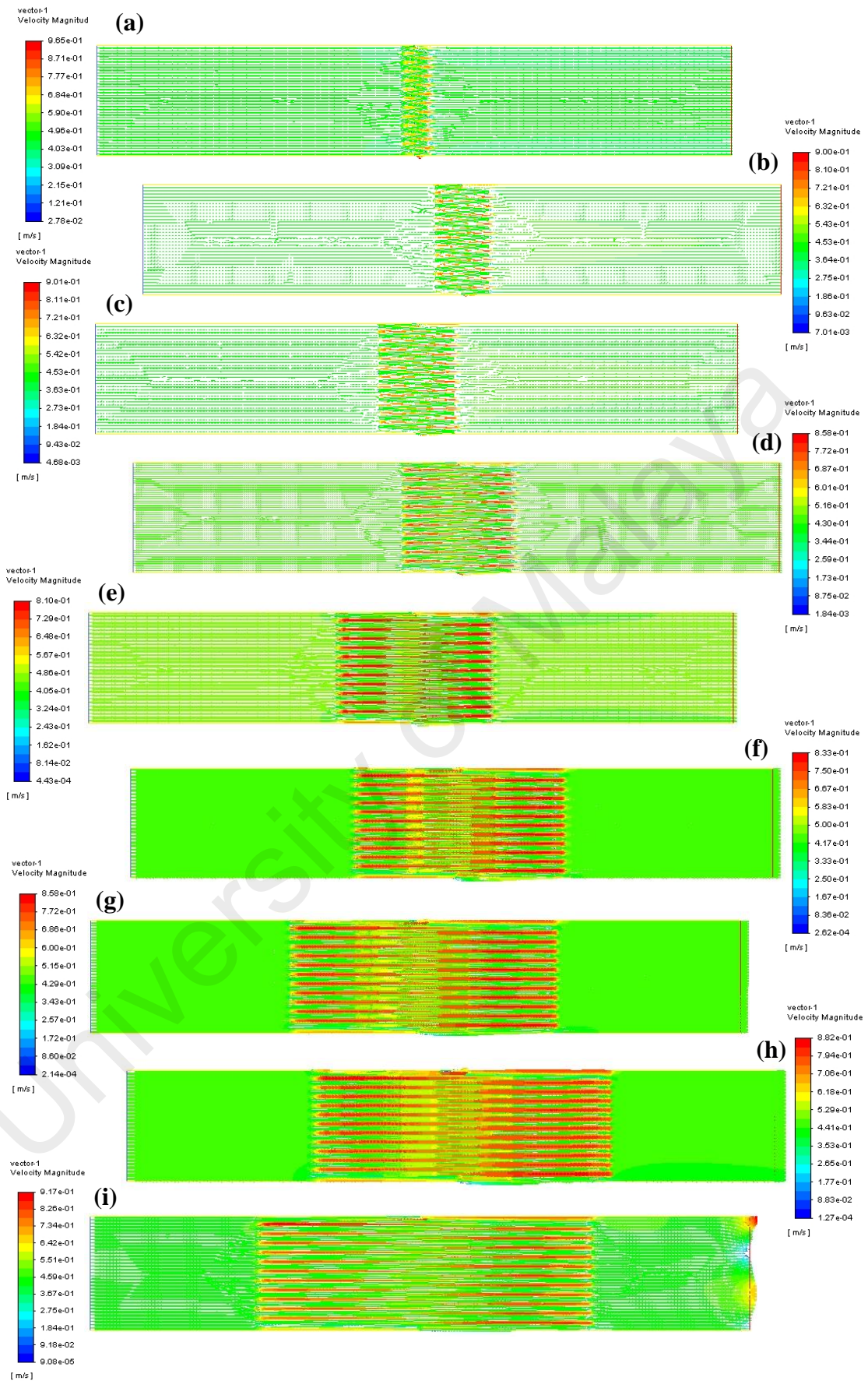


Figure 4.11: Velocity vectors of the air flow across filter media pack with pleat depth of (a) 12 mm, (b) 25 mm, (c) 35 mm, (d) 50 mm, (e) 70 mm, (f) 95 mm, (g) 120 mm, (h) 135 mm, and (i) 150 mm.

is a threshold in the angle of the filter media and beyond this threshold shows no significant changes.

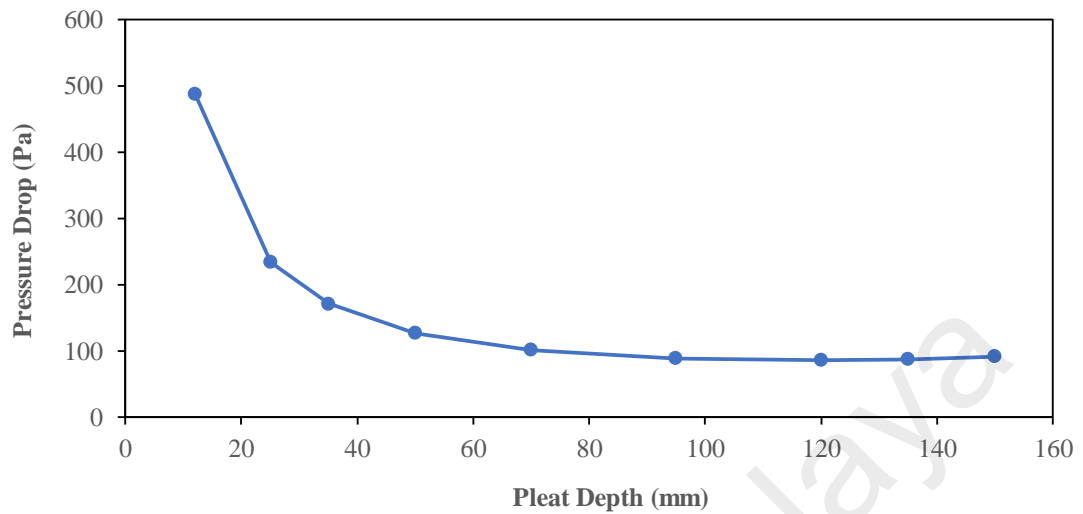


Figure 4.12: Graph of pressure drop predictions against pleat depth of filter media packs.

4.4 Chapter Conclusions

In this chapter, the parametric studies on the dimensions of the filter media pack was investigated. It is shown that increasing the amount of space available for the air flow would decrease the pressure drop across the filter media. However, due to the impracticality of building an air filter that is indefinitely large, filter manufacturers resolve to folding the filter media into a filter media pack to decrease the pressure drop of the air filter and still meeting the space constraints. For the filter media pack dimensions, there is an optimum region whereby outside of this region would either have undesirable effects or insignificant changes. The suggested optimum dimension of the Filter Media Pack is to have a Pleat Depth of 120mm and a Pleat Density of 6 PPI.

CHAPTER 5: 3-D CFD SIMULATIONS

5.1 Introduction

As a continuation from the results obtained in Chapter 4, the optimum dimensions of the Filter Media Pack were analyzed in this chapter with 3-D CFD simulations. Firstly, a total of three models of 3-D pleated filter media are introduced in Section 5.1. In Section 5.2, the computational results for all the 3-D CFD simulations are reported. Then, the filtration performance of each design is compared and discussed in Section 5.4. Lastly, the findings obtained in this study are summarized in Section 5.5.

5.2 3-D Pleated Filter Media Models

A total of three filter media packs were modeled for the CFD simulation, as illustrated in Figure 5.1. The dimensions of all three media pack are 6 PPI and 120mm Pleat Depth, as per the findings from Chapter 4. The media pack is fitted into a 50mm × 50mm cross section duct with a total length of 250mm. These three models are denoted as below:

- i) An ideal media pack,
- ii) Media pack with hotmelt adhesives, and
- iii) Media pack with emboss design.

The ideal media pack is simply a flat sheet of filter media pleated into the desired media pack dimensions. In practice, the ideal media pack could be manufactured, but it is not feasible to be assembled into an air filter. This is because without any form of adhesive for the media pack to maintain its pleated shape, the filter media would be blown out of its frame when subjected to an air flow.

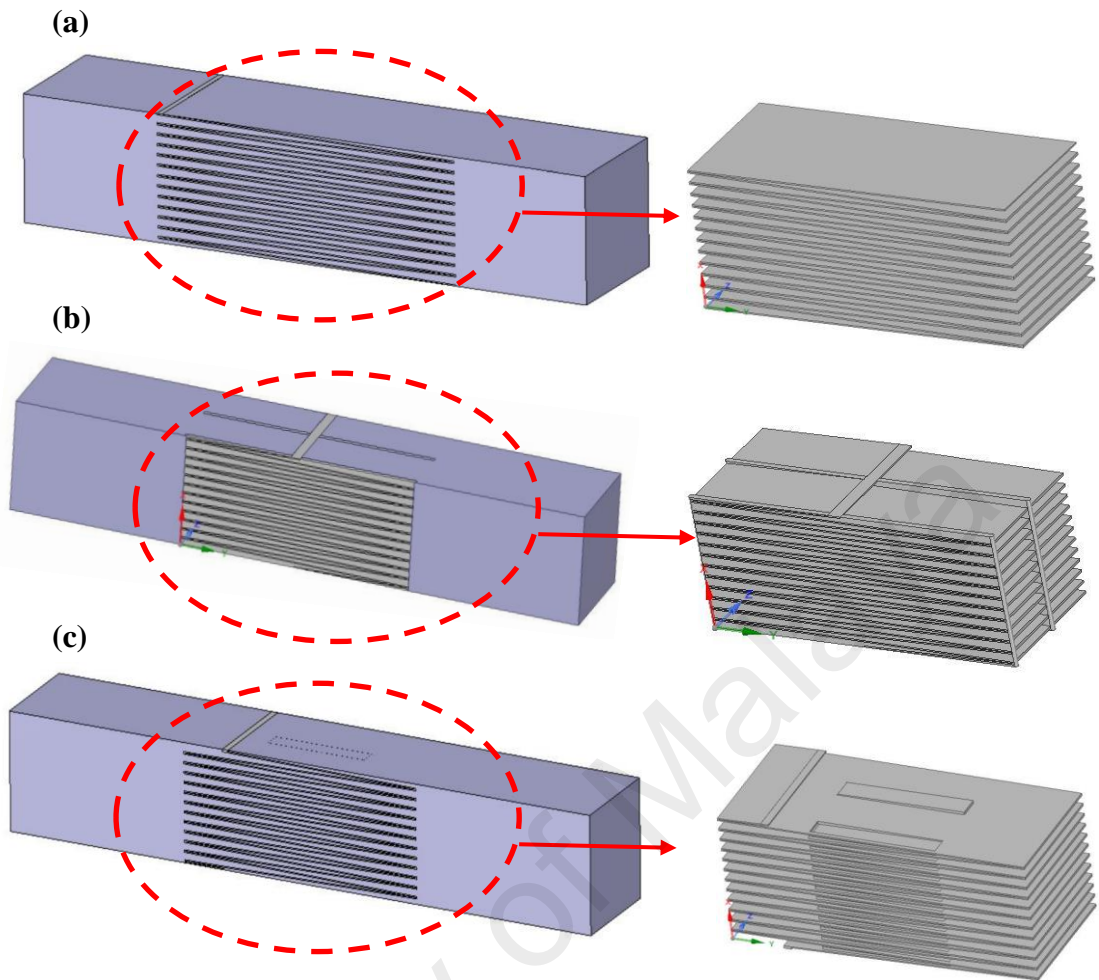


Figure 5.1: 3-D pleated filter media models (a) of an ideal media pack, (b) a media pack with hot-melt adhesive layer, and (c) with emboss design.

Hence, filter manufacturers apply thin lines of hotmelt adhesives to ensure the pleat shapes stays in place when subjected to an air flow. The model for a practical form of media pack is shown in Figure 5.2. The same specifications as the ideal media pack were used, but two lines of hotmelt adhesives were added to the model. The hotmelt adhesives were modeled as a 2mm thick solid across the entire depth of the media pack and they were spaced 25mm apart. This spacing distance is commonly used by air filter manufacturers. These hotmelt layers are highlighted in blue colour in Figure 5.2 for illustration purposes only, in practice it is usually white in colour.

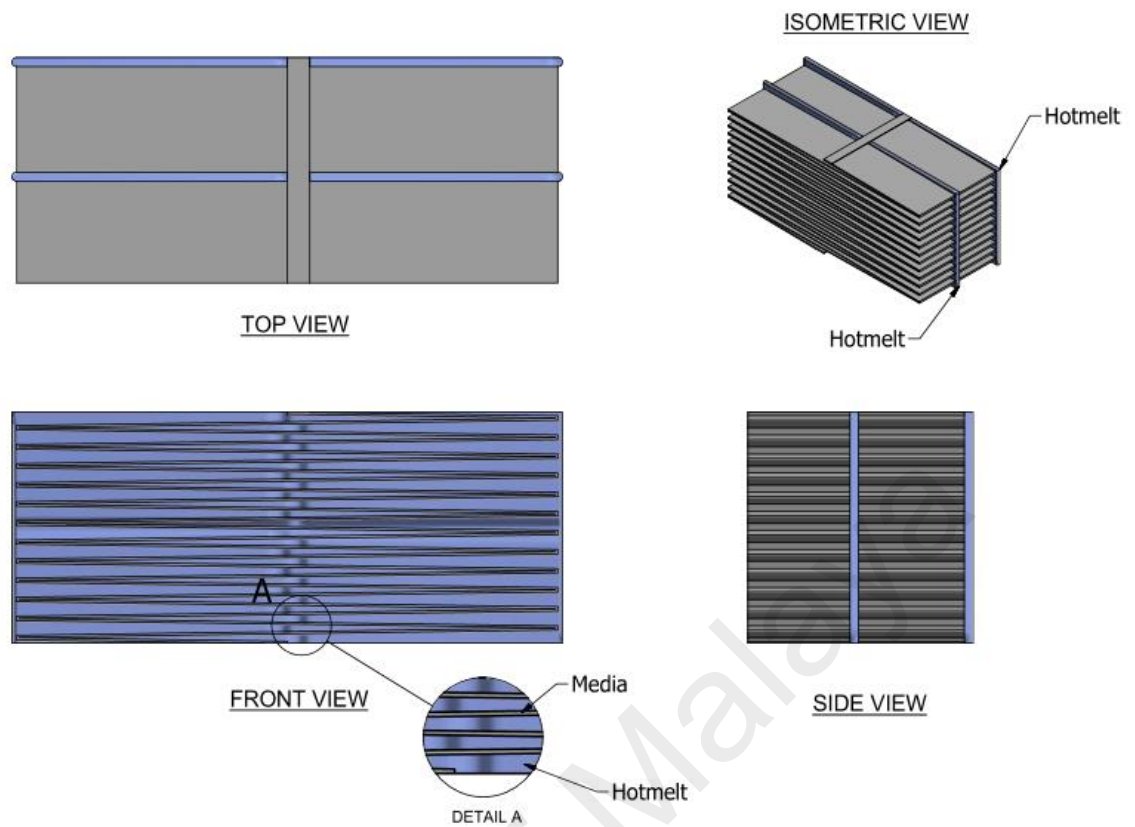


Figure 5.2: The 3-D model of the media pack with 2 layers of hotmelt adhesive.

Finally, the model of the media pack with the emboss design is shown in Figure 5.3. An emboss of 80mm length and 10mm wide is added to the media pack. The embossment are spaced 25mm apart also. It is important to note that the embossment direction alternates between inwards and outwards, this is so that the media pleats are supported at both the upstream and the downstream portion for it to maintain its shape. Also, the embossments are slanted at an angle such that opposing embossment will meet at a horizontal position, for the pleats to maintain its angle. In practice, there will be a small amount of adhesive applied to the surface of the embossment to keep the media pack in place. However, this is not considered in the model due to the limited processing capabilities available for this project. Moreover, it is more worthwhile to first investigate the performance of the emboss media pack without the effects of the glue, before determining the necessity to include the aforementioned effects in the future work.

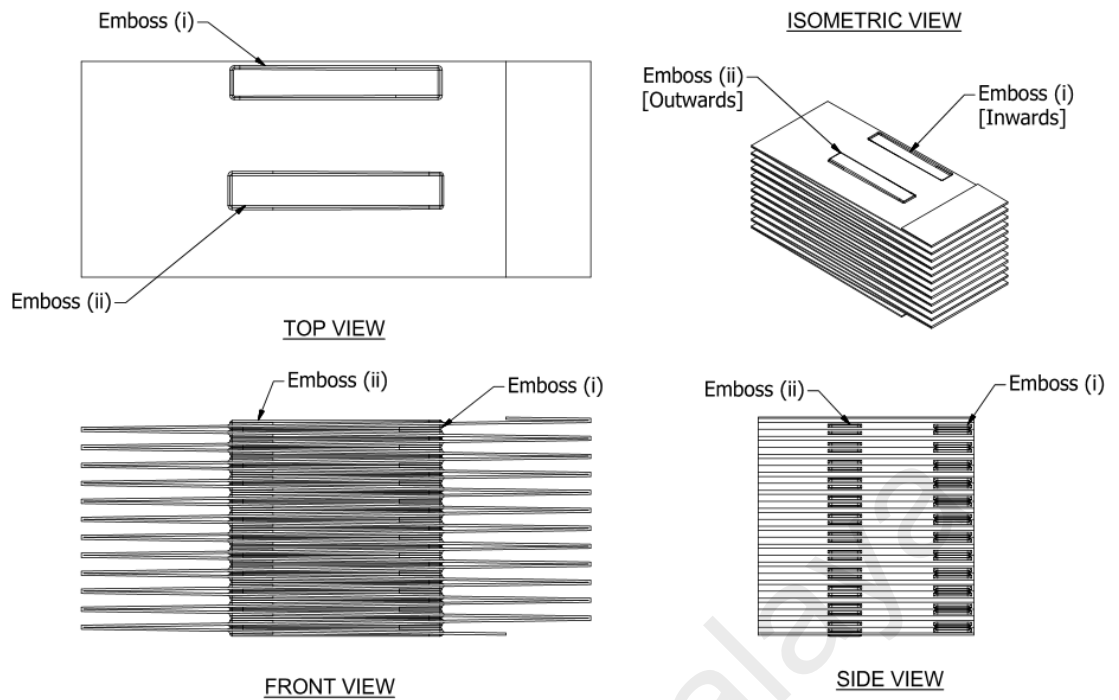


Figure 5.3: The 3-D model of the media pack with emboss design.

5.3 Computational Results for 3-D Simulations

For all the 3 models mentioned in Section 5.2, the inlet velocity is set at 0.45 m/s. This inlet velocity is consistent with the 2-D simulation reported in Chapter 4. In addition, the filter media is set as a porous medium with the permeability values used from the 2-D models. All 3 models were analyzed by computing the pressure and velocity profile along the duct.

5.3.1 Ideal Media Pack Model

For the ideal media pack model, the pressure difference across the media pack is computed to be 87 Pa, as shown in Figure 5.1. The pressure difference for the corresponding 2-D model is 85.6 Pa, as reported in Chapter 4. Therefore, the differences between the 3-D and 2-D models are less than 2%, which is sufficient to confirm the validity of the 3-D model.

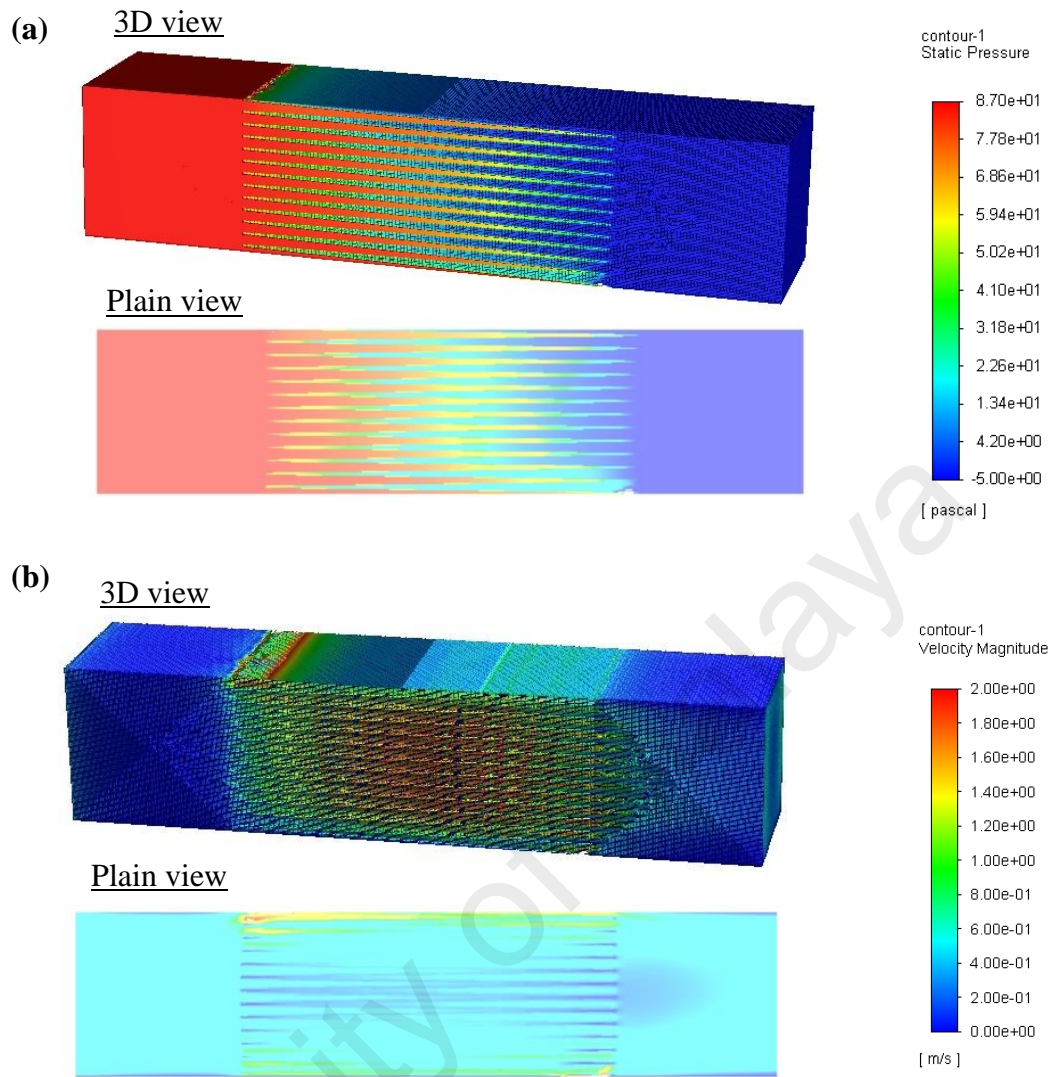


Figure 5.4: (a) Pressure drop and (b) velocity profile predictions across simple pleated filter media model.

5.3.2 Pleated Filter Media Model with Hot-Melt Layers

Next, 2 lines of hotmelt adhesive were added to the model and they were set as solids. The pressure and velocity profile of the model are presented in Figure 5.5. It can be observed that the pressure difference across the media pack is increased to 120 Pa, which is a 38% increment. This is expected as the hotmelt layers present a solid obstruction to the air flow. From the velocity profile shown in Figure 5.5(b), there is an increase in the velocity at the starting tip of the media pack, this indicates that the obstruction from the hotmelt layers caused a reduce in cross section area for the air to flow through.

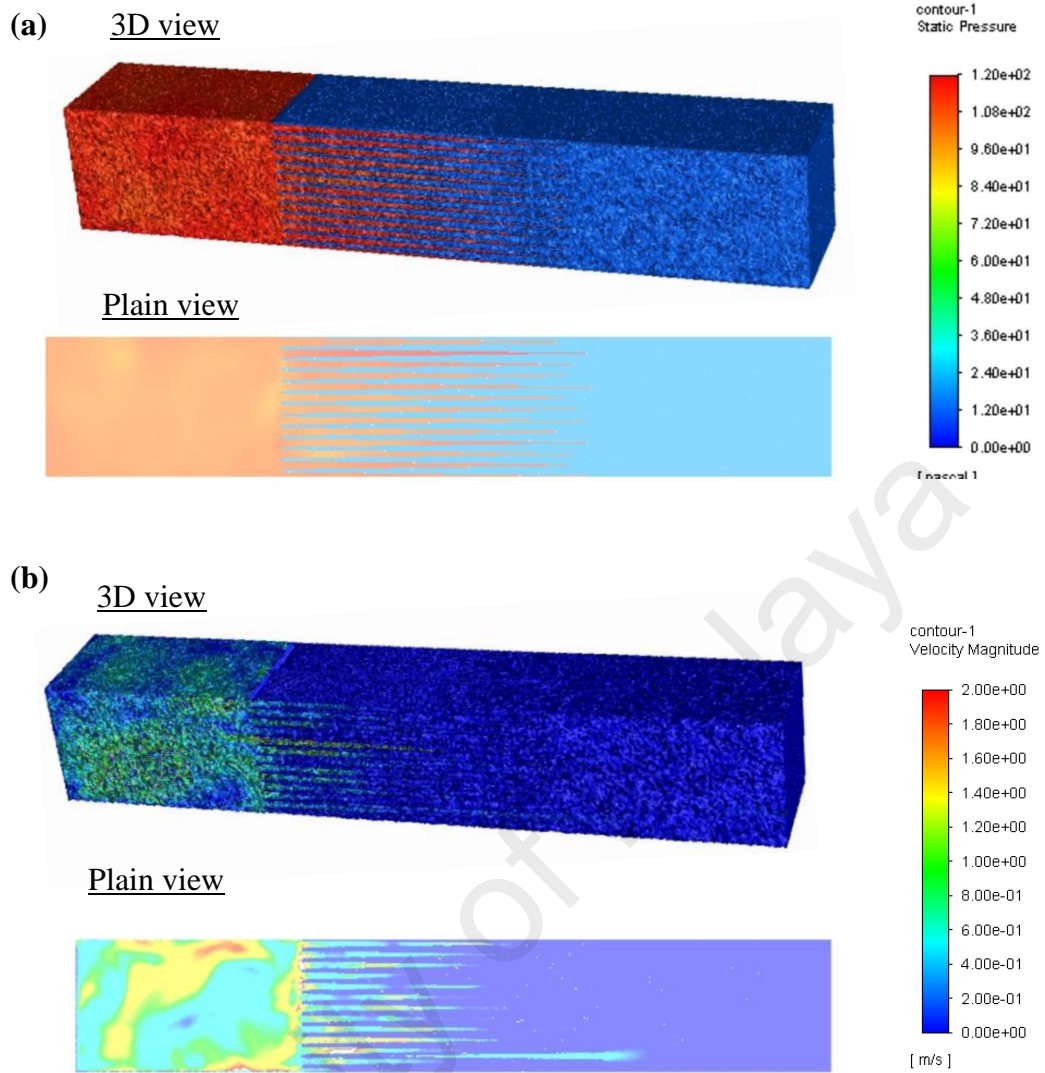


Figure 5.5: (a) Pressure drop and (b) velocity profile predictions across pleated filter media model with hot-melt layers.

Therefore, the effects of adding the hotmelt layers is significant when evaluating the performance of a media pack.

5.3.3 Pleated Filter Media Pack Model with Emboss Design

Finally, the model for the media pack with emboss design was analysed and the pressure and velocity profile were presented in Figure 5.6. Similar to the aforementioned models in this Chapter, there is a high pressure region at the upstream of the media pack and the pressure gradually decrease along the media pack before finally a low pressure region is formed at the downstream of the media pack. The total pressure decrease is 108

Pa. For the velocity profile, there is an increase in velocity at the embossment region, which is expected as the embossment present a constriction to the air flow.

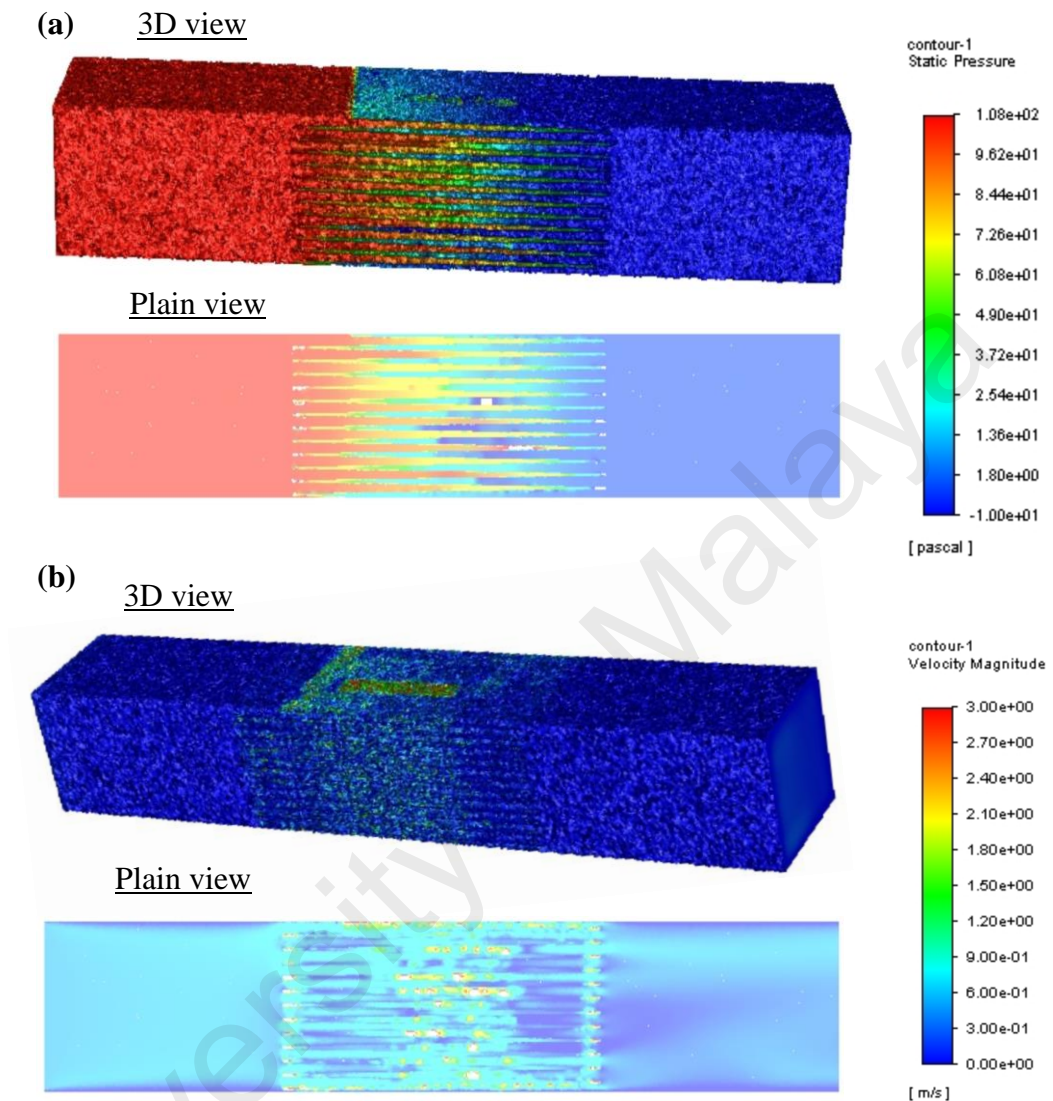


Figure 5.6: (a) Pressure drop and (b) velocity profile predictions across pleated filter media model with emboss design.

5.4 Discussions on the Filtration Performance of the Various Designs

Based on the results of the 3-D simulation, the resistance to air flow of all 3 media packs are summarized and compared in Table 5.1. Comparisons percentage increase in the resistance to air flow are made for the media pack with hotmelt and media pack with emboss against the ideal media pack.

Table 5.1: Filter media pack resistance to air flow comparison against the Ideal Media Pack

Description	Resistance to Air Flow (Pa)	Comparison Against Ideal Media Pack
Ideal Media Pack	87	-
Media Pack with Hotmelt	120	+ 38 %
Media Pack with Emboss	108	+ 24 %

Referring to Table 5.1, both the media pack with hotmelt and media pack with emboss have a higher resistance to air flow as compared to the ideal media pack. This is expected as both the hotmelt and the emboss features presents a disruption to the air flow. Once again, it is important to highlight that the hotmelt layers are necessary for the media pack to maintain its shape when subjected to air flow. In a similar manner, the embossment also serves as a method to keep the filter media pack in place. Set against this background, the resistance to air flow of both the media pack with hotmelt and media pack with emboss are compared against the ideal media pack. From the comparison made in Table 5.1, the resistance to air flow of the media pack with hotmelt is higher than that of the media pack with emboss. This is due to the hotmelt being a solid obstruction to the air flow and the air is required to navigate pass the hotmelt layer. On the other hand, the embossment is still a porous medium which allows air to pass through. In addition, as illustrated in Figure 5.2, the hotmelt regions stretches the entire length of its media pack and it occurs both at the upstream and downstream of the media pack. In contrast, as shown in Figure 5.3, the embossment feature is only at the centre region of the media pack. The edges of the media pack still resemble the ideal media pack. On top of that, the embossment direction alternates between inwards and outwards to provide support for both upstream and downstream region, as opposed to the hotmelt feature whereby every hotmelt layers occurs at both upstream and downstream region. Therefore, the media pack with the hotmelt layers posses more resistance to the air flow as compared to the media pack with emboss design.

5.5 Chapter Conclusions

In this chapter, the results of the 3-D simulations were presented and discussed. A total of three 3-D models were constructed, which is the Ideal Media Pack, the Media Pack with Hotmelt Layers and the Media Pack with Emboss design. It is found that the Media Pack with Hotmelt Layers has a 38% increase in resistance to air flow as compared to the Ideal Media Pack. In contrast, the Media Pack with Emboss design has a 24% increase in resistance to air flow as compared to the Ideal Media Pack. This shows that the Media Pack with Emboss design is a better design as compared to the Media Pack with Hotmelt Layers as it has a lower resistance to air flow.

University of Malaya

CHAPTER 6: COST ANALYSIS

6.1 Introduction

In this chapter, the cost analysis of the emboss filter pack is presented. The analysis begins with comparing the manufacturing cost to produce a filter media pack with hotmelt layers and an emboss filter media pack. Then, the improvement of filter specifications due to the emboss filter media pack is evaluated. This evaluation is essential to provide a forecast on the selling price of a filter with emboss media pack. Consequently, the Return of Investment (ROI) of manufacturing a filter with emboss media pack is evaluated. Lastly, a summary on the cost analysis is provided in the last section of the chapter.

6.2 Manufacturing Cost

The total manufacturing cost of an air filter can be split into two parts, which are the material cost and the cost of the manufacturing process. A comparison between both costs for the media pack with hotmelt layers and emboss media pack is made. The size of the media pack dimensions was chosen as 610 mm Width \times 610 mm Height \times 120 mm Depth. The 120 mm Depth was chosen based on the optimum Pleat Depth of the media pack, as discussed in Chapter 4. The cross-section size of 610 mm Width \times 610 mm Height was chosen because this is a commonly used size of an air filter for Heating, Ventilation and Air Conditioning (HVAC) applications. The Computer Aided Design (CAD) models of both media pack is shown in Figure 6.1. The following subsections discusses in detail the material cost and manufacturing process cost of both media packs.

6.2.1 Materials Cost

The materials required to manufacture air filters using both media packs are compared and summarized in Table 6.1. For the filter frame, both media packs can be fitted into the same filter frame as it can be made into the same external dimensions. There are many

options for air filter frames material, ranging from Galvanized Steel to plastic extrusion, depending on its application, site and customers' requirements. Therefore, the material cost contributed from the filter frame is the same for both media packs design.

Next, the media material used to produce both media packs are fiberglass sheets. The cost of the fiberglass sheets contributes the most to the overall material cost of an air filter. Both media packs require the same amount of fiberglass sheets to produce the same media pack dimensions. The embossing of the media pack with emboss design do not require additional amount of fiberglass material as the emboss can be made using an emboss tool to press on the fiberglass media sheet. The fiberglass media has a 0.5 mm thickness and it can be stretched slightly to create the embossment without breaking. Consequently, the stretched region will be thinner than 0.5 mm.

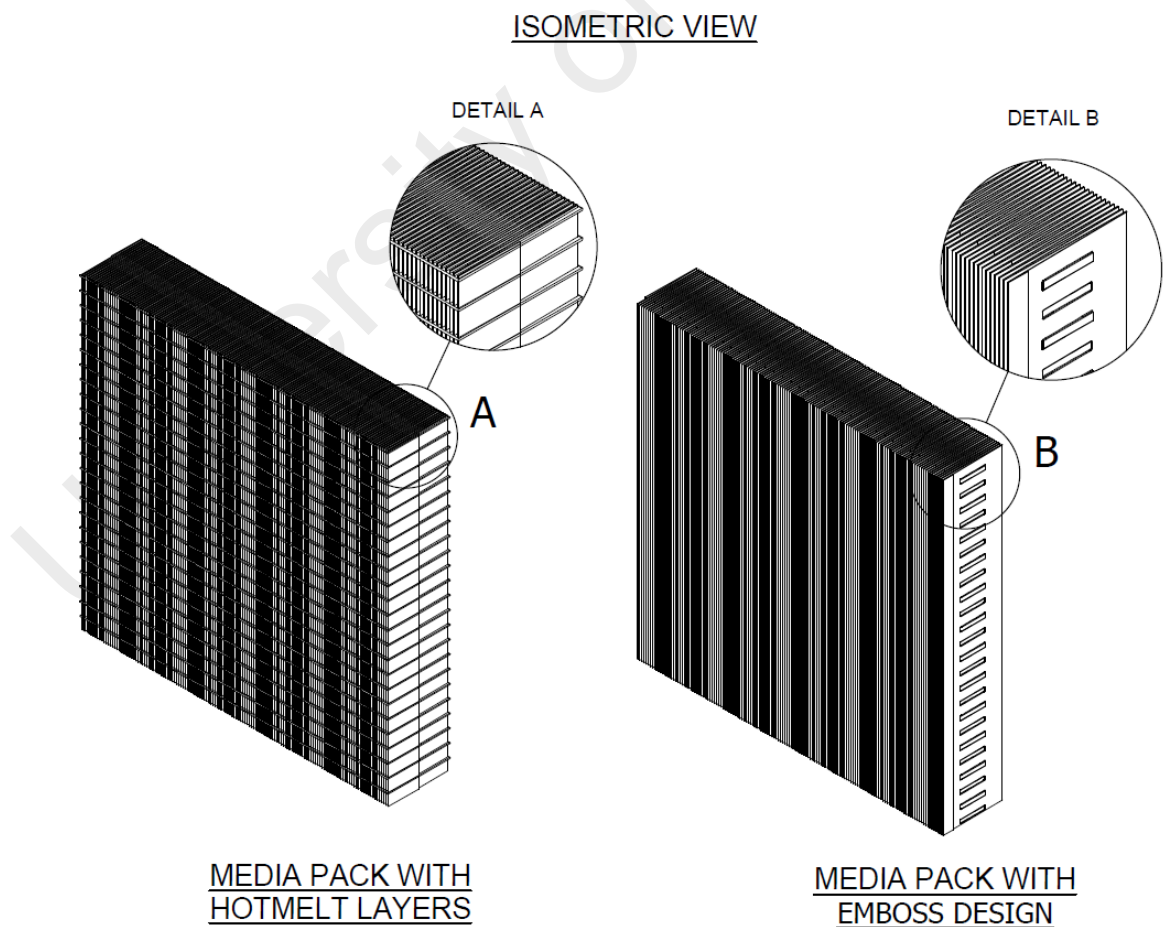


Figure 6.1: Computer Aided Design (CAD) Models of the Media Pack with Hotmelt Layers and Media Pack with Emboss Design.

After the media pack is placed in the filter frame, the contacting surfaces between the filter frames and media pack are required to be sealed off to avoid bypass of air flow. Again, there are many options for the sealant used depending on the filter grade, application, site and customer requirement. Despite that, both media packs can be sealed off with the same type and amount of sealant. Next, the packaging materials for filters with both types of media pack are the same as well. Good quality air filters are packed in plastic bags and placed in carton boxes with shock absorption materials. This is to ensure the fiberglass media will not be damaged during transportation. Hence, the same packaging methods and material required can be applied to both air filter with hotmelt layers and with emboss design.

Lastly, the only difference in materials used between both media packs are the usage of the hotmelt and the glue. As stated in Chapter 5, the media pack with emboss design requires a small amount of glue at the mating surfaces of the embossment to keep the media pack intact and maintain its pleated shape when subjected to airflow. The usage of glue instead of hotmelt for the media pack with emboss design is able to reduce the overall material cost of the air filter by up to 15%. This is dependent on the specifications of the filter as it will affect the material selection and, consequently, the cost for the other parts.

Table 6.1: Summary of the Materials Required to Manufacture Air Filters with the Media Pack with Hotmelt Layers and Media Pack with Emboss Design

Materials	Media Pack with Hotmelt Layers	Media Pack with Emboss Design
Filter Frame	✓	✓
Fiberglass Media	✓	✓
Hotmelt	✓	-
Glue	-	✓
Sealant	✓	✓
Packaging Materials	✓	✓

As a result, it can be estimated that the material cost for producing the media pack with emboss design is 15% lesser than that for the media pack with hotmelt layers.

6.2.2 Manufacturing Process

After analyzing the material cost, the next cost analysis required is on the manufacturing process. A comparison between the manufacturing process to produce an air filter with the media pack with hotmelt layers and media pack with emboss design is made and presented in Figure 6.2.

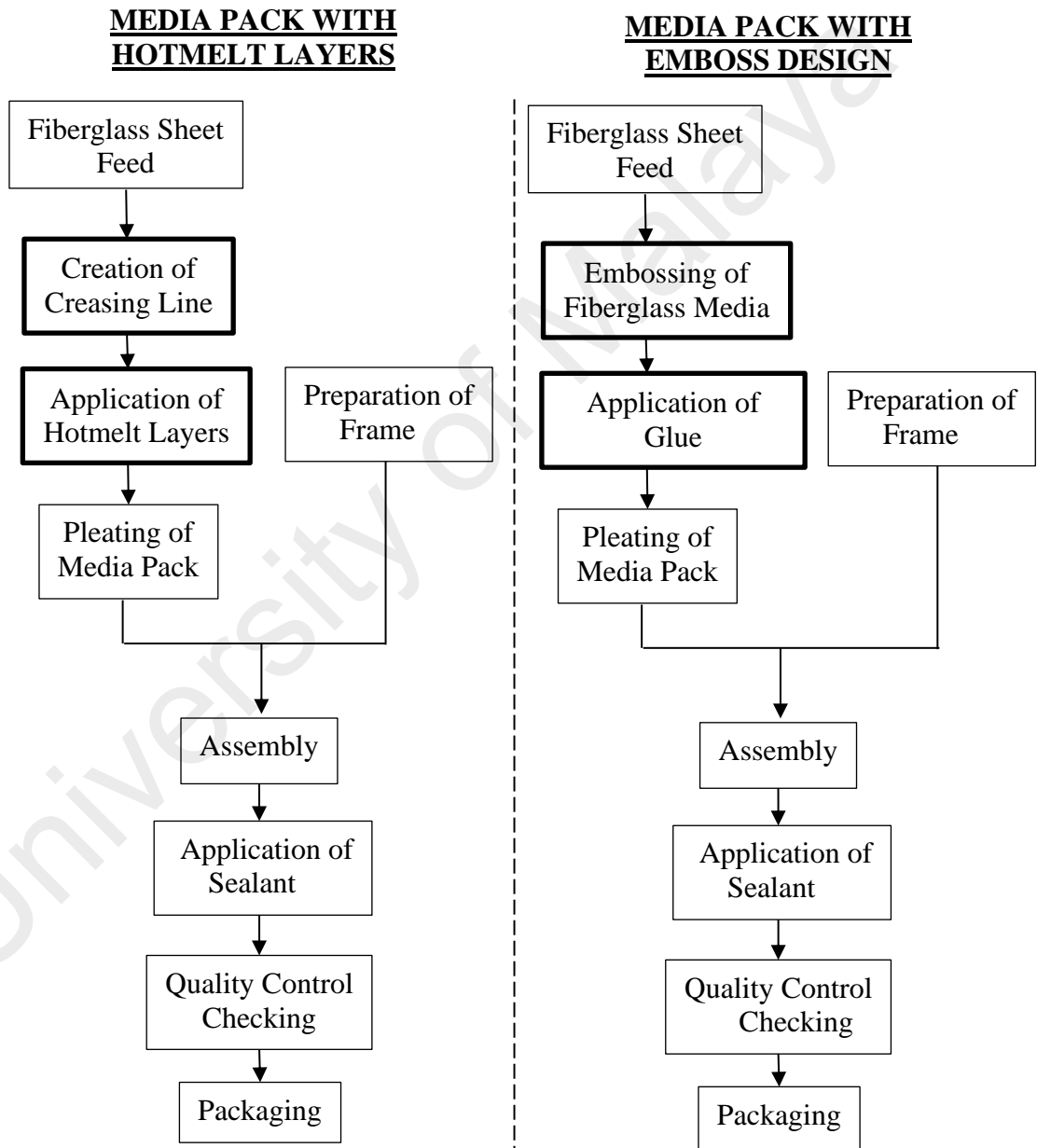


Figure 6.2: Comparison of the Manufacturing Processes to produce an air filter with media pack with hotmelt and media pack with emboss design.

Referring to Figure 6.2, only two processes are different to produce an air filter with the different media pack designs, as highlighted in the Bold Line box. The creation of creasing line is a process whereby a minor indentation is made on the surface of the fiberglass media sheet to allow the sheet to be pleated into a media pack. For the media pack with emboss design, the creation of creasing line can be incorporated into the embossing tool. Due to this, there is no need for a separate process to create the creasing line. For the application of the hotmelt layers and the glue, the same tools may be used by just changing the adhesive materials. The tools are electronically controlled, thus, the settings may be changed to vary the amount of glue or hotmelt applied. For the other processes, no further modifications or changes are required.

Apart from that, the time taken for every process are analyzed as well, as this will affect the overall production rate. For the processes that are not highlighted in bold in Figure 6.2, the time taken to complete these processes are the same as there is no changes or modifications to these processes. Besides that, the time taken for the application of hotmelt or glue are the same as well as only the feed material is changed, but the tooling remains unchanged. However, the creation of crease line takes a lesser time as compared to the embossing of the media. It is estimated that for a full production day of 9 hours, the production rate of the filters with emboss media pack is 20% slower than that of the filters with media pack with hotmelt layers.

Therefore, the manufacturing process cost is higher to produce an air filter with emboss media pack, due to the slower production rate.

6.3 Improvement of Specifications

In addition to the manufacturing cost, the overall cost analysis takes into account on the improvement of specifications of the air filter with the emboss media pack. This is important as it will affect the potential selling price of the air filter. From Chapter 2, the

specifications to assess the performance of an air filter are the Resistance to Air Flow, the Dust Holding Capacity and the Filtration Efficiency. These three specifications are evaluated in this section.

From the CFD simulations results in Chapter 4 and Chapter 5, it was predicted that the emboss media pack has a 10% lower resistance to air flow as compared to the media pack with hotmelt layers. This lower resistance is significant as it will improve the energy consumption rating of the air filter (Certita, 2018). Besides that, air filter manufacturers recommend the service life of air filters based on the resistance to air flow of the air filter. As an air filter collects dust from the air stream, the porosity of the filter media will decrease as the dust are blocking the air passages. This will cause an increase in resistance to air flow. When the resistance to air flow of the air filter reaches the recommended value by its manufacturer, then the air filter is required to be replaced. Therefore, a lower initial resistance will help to prolong the service life of the air filter.

Next, the Dust Holding Capacity of the air filter with the media pack with hotmelt layers and media pack with emboss design is evaluated. The Dust Holding Capacity of an air filter is directly related to the filter media surface area. This is because more media surface area would allow more space for dust to be captured. From the CAD models shown in Figure 6.1, the total surface area of both media packs is calculated. It is found that the surface area of the media pack with emboss design is 12% higher than that of the media pack with hotmelt layers. Consequently, it can be estimated that an air filter with media pack with emboss design has a 12% higher Dust Holding Capacity.

Finally, the filtration efficiency is dependent on the grade of fiberglass media used. Hence, both designs of the media pack have no effects on this specification.

6.4 Return of Investment (ROI)

To relate all the aforementioned cost analysis, the Return of Investment (ROI) of developing an air filter with media pack with emboss design is estimated. A recap of the results of the aforementioned cost analysis is provided in Table 6.2.

Table 6.2: Comparison of the Air Filter with Media Pack with Emboss Design versus Media Pack with Hotmelt Layers.

Description	Comparison of an Air Filter with Media Pack with Emboss Design versus the Media Pack Hotmelt Layers.
<i>Manufacturing Cost</i>	
Material Cost	-15%
Manufacturing Process Cost	+20%
<i>Improve of Specifications</i>	
Resistance to Air Flow	-10%
Dust Holding Capacity	+ 12%
Filtration Efficiency	-

Referring to Table 6.2, the additional manufacturing process cost to produce the air filter with media pack with emboss design can be offset by the reduction in material cost. Generally, the ratio of Material Cost to Manufacturing Process Cost of an air filter is approximately 8:2. Therefore, a 15% reduction in material cost would be more than the 20% increase in manufacturing process cost. Overall, this would give an 8% reduction in manufacturing cost.

Furthermore, the air filter with media pack with emboss design has superior performances, as its resistance to air flow is lower and its dust holding capacity is higher. This would allow the air filter manufacturer to price the filter at a higher price range.

However, the ROI analysis also takes into account the additional investment needed to acquire the tools to make the embossment. It is estimated that the acquisition cost for the embossing tools are RM 5,000. Hence, an air filter manufacturer would need to invest

up to RM 5,000 in the initial stage, before being able to benefit from the lower manufacturing cost and higher selling price of the air filter with emboss filter media pack. The air filter manufacturer could also consider the option to amortize the initial investment over a period of sales of the air filter with emboss filter media pack. This depends on the potential sales volume that the air filter manufacturer is capable to achieve.

Overall, the cost analysis for developing an air filter with media pack with emboss design shows that there is potential for high ROI.

6.5 Chapter Conclusions

In this chapter, a cost analysis for developing an air filter with the media pack with emboss design is performed. It is found that the manufacturing cost of such air filter is lower than that of the air filter with media pack with hotmelt layers. In addition to that, the specifications of the performance of the air filter with the media pack with emboss design is better than the air filter with media pack with hotmelt layers. Lastly, it is concluded that there is potential for high ROI in developing the air filter with the media pack with emboss design.

CHAPTER 7: CONCLUSIONS AND FUTURE WORK

7.1 Conclusions

In this work, the feasibility of developing an embossed fiberglass filter media pack for air filtration devices are investigated. The investigation was carried out by analysing the increase in performances of a filter media pack with emboss design. The analysis involves performing 2-D and 3-D CFD simulation models. With the results from the CFD simulation models, a cost analysis was performed to evaluate the ROI of developing an air filter with media pack with emboss design.

From this work, the following conclusions were made:

- There is an optimum dimension when manufacturing a filter media pack. The optimum is to have a 120mm Pleat Depth and 6 PPI pleat density,
- The air filter with media pack with emboss design is able to achieve better air filter performances. Its resistance to air flow is lower and its dust holding capacity is higher when compared to the commonly manufactured air filters.
- The manufacturing cost to produce an air filter with media pack with emboss design is lower when compared to an equal dimensions and specifications air filter.
- There is potential for high ROI in developing an air filter with media pack with emboss design.

Lastly, it is concluded that it is feasible to develop an air filtration device with an embossed Fiberglass Media. Furthermore, developing such an air filtration device will help in increasing the boundaries of air filter performances as well as producing air filters that consumes less energy. This provides an opportunity to develop a more energy efficient system that is capable of providing better air quality.

7.2 Recommendations for Future Work

Based on the findings obtained in this study, recommendations are made to encourage further improvement to the research and development of producing air filtration devices with an embossed Fiberglass media pack, as listed below:

- The CFD simulations can be repeated for other flat sheet media specifications. In this study, the media used has a 0.5mm thickness and 250 Pa air resistance at 5.3 cm/s air velocity. Other flat sheet specifications will have a different optimum media pack dimension.
- The effects of adding glue to the embossment surface is also recommended to be investigated.
- Methods to develop CFD simulation model for dust holding capacity of an air filtration devices.

University of Malaya

REFERENCES

- Bull, K., & Roux, P. (2010). Cabin air filtration systems-novel technological solutions for commercial aircraft. In *40th International Conference on Environmental Systems* (p. 6291).
- Chen, D.-R., Pui, D. Y. H., & Liu, B. Y. H. (1995). Optimization of pleated filter designs using a finite-element numerical model. *Aerosol Science and Technology*, 23(4), 579–590.
- Certita, E. (2018). AIR FILTERS - New energy efficiency classification for 2019. Retrieved from <https://www.eurovent-certification.com/en/company-news/AIR-FILTERS-New-energy-efficiency-classification-for-2019>
- Del Fabbro, L., Laborde, J. C., Merlin, P., & Ricciardi, L. (2002). Air flows and pressure drop modelling for different pleated industrial filters. *Filtration & Separation*, 39(1), 34–40.
- Domnița, F., Bacoțiu, C., Hoțupan, A., Popovici, T., & Kapalo, P. (2014). Study on Mechanical Separation of Dust using Louver Type Inertial Separator. *Journal of Applied Engineering Sciences*, 19.
- Feng, Z., Long, Z., & Chen, Q. (2014). Assessment of various CFD models for predicting airflow and pressure drop through pleated filter system. *Building and Environment*, 75, 132–141.
- Ferziger, J. H., & Perić, M. (2002). *Computational methods for fluid dynamics* (Vol. 3). Springer.
- Fluent, A. (2015). Theory guide. *Ansys Inc.: Canonsburg, PA, USA*.

- Fotovati, S., Hosseini, S. A., Tafreshi, H. V., & Pourdeyhimi, B. (2011). Modeling instantaneous pressure drop of pleated thin filter media during dust loading. *Chemical Engineering Science*, 66(18), 4036–4046.
- Fu, H. M., Fu, Y., & Xu, F. (2014). Experiment and simulation on pressure drop of pleated air filters. In *Advanced Materials Research* (Vol. 960, pp. 568–573). Trans Tech Publ.
- GmbH, E. filtertechnik. (n.d.). Theory of particle filtration. Retrieved from <https://www.emw.de/en/filter-campus/theory-of-particle-filtration.html>
- Goodfellow, H. D. (2001). *Industrial ventilation design guidebook*. Elsevier.
- Gopani. (n.d.). Gopani: Cartridge Filter. Retrieved from <https://www.gopani.com/what-is-cartridge-filter/>
- Gras, J. L. (1994). Air filtration: An integrated approach to the theory and applications of fibrous filters [Book Review]. *Clean Air: Journal of the Clean Air Society of Australia and New Zealand*, 28(4), 42.
- Hutten, I. M. (2007). *Handbook of nonwoven filter media*. Elsevier.
- Legg, R. (2017). *Air Conditioning System Design*. Butterworth-Heinemann.
- Liu, B. Y. H., Rubow, K. L., & Pui, D. Y. H. (1985). Performance of HEPA and ULPA Filters. In *Proceedings, Annual Technical Meeting-Institute of Environmental Sciences*. Inst of Environmental Sciences.
- Mohan, B., Yang, W., & Chou, S. K. (2013). Fuel injection strategies for performance improvement and emissions reduction in compression ignition engines—A review. *Renewable and Sustainable Energy Reviews*, 28(x), 664–676.

Purchas, D., & Sutherland, K. (2002). *Handbook of filter media*. Elsevier.

Qian, F., Huang, N., Lu, J., & Han, Y. (2014). CFD–DEM simulation of the filtration performance for fibrous media based on the mimic structure. *Computers & Chemical Engineering*, 71, 478–488.

Roache, P. J. (1998). *Fundamentals of computational fluid dynamics*. Albuquerque, NM: Hermosa Publishers, 1998.

Schousboe, F. C., & Schousboe, F. C. (2017). Media Velocity Considerations in Pleated Air Filtration.

Tronville, P., & Rivers, R. D. (2005). International standards: filters for buildings and gas turbines. *Filtration & Separation*, 42(7), 39–43.

Tronville, P., & Sala, R. (2003). Minimization of resistance in pleated-media air filter designs: empirical and CFD approaches. *HVAC&R Research*, 9(1), 95–106.

Tsang, C. M. (1999). *Analysis of pleated air filters using computational fluid dynamics*. University of Toronto.

Tu, J., Yeoh, G. H., & Liu, C. (2018). *Computational fluid dynamics: a practical approach*. Butterworth-Heinemann.

Van der Smissen, C.-E. (1987). Filter comprising a catalyst on a substrate for purification of air. Google Patents.

Wang, Y., Brannock, M., Cox, S., & Leslie, G. (2010). CFD simulations of membrane filtration zone in a submerged hollow fibre membrane bioreactor using a porous

media approach. *Journal of Membrane Science*, 363(1–2), 57–66.

White, E. (2009). HEPA and ULPA filters. *Journal of Validation Technology*, 15(3), 48–55.

Xu, H., Jin, W., Wang, F., Li, C., Wang, J., Zhu, H., & Guo, Y. (2018). Preparation and properties of PTFE hollow fiber membranes for the removal of ultrafine particles in PM 2.5 with repetitive usage capability. *RSC Advances*, 8(67), 38245–38258.

Yue, C., Zhang, Q., & Zhai, Z. (2016). Numerical simulation of the filtration process in fibrous filters using CFD-DEM method. *Journal of Aerosol Science*, 101, 174–187.

University of Malaya